Vol. 74, Part I, 2004

ISSN 0369-8211

Proceedings of the National Academy of Sciences India

SECTION A — PHYSICAL SCIENCES

National Academy of Sciences, India, Allahabad
राष्ट्रीय विज्ञान अकादमी, भारत, इलाहाबाद

The National Academy of Sciences, India

(Registered under Act XXI of 1860)

Founded 1930

COUNCIL FOR 2004

President

1 Prof Jai Pal Mittal, Ph D (Notre Dame), F N A , F A Sc , F N A Sc , F T W A S , Mumbai

Two Past Presidents (including the Immediate Past President)

2 Prof S K Joshi, D Phil , D Sc (h c), F N A , F A Sc , F N A Sc , F T W A S , New Delhi

3 Dr V P Sharma, D Phil ,D Sc ,F A M S ,F E S I , F I S C D , F N A , F A Sc , F N A Sc , F R A S , New Delhi

Vice-Presidents

4 Dr P K Seth, Ph D , F N A , F N A Sc , Lucknow

5 Prof M Vijayan, Ph D , F N A , F A Sc , F N A Sc , F T W A S , Bangalore

Treasurer

6 Prof S L Srivastava, D Phil ,F I E T E , F N A Sc , Allahabad

Foreign Secretary

7 Dr S E Hasnain, Ph D , F N A , F A Sc , F N A Sc , F T W A S , Hyderabad

General Secretaries

8 Dr V P Kamboj, Ph D , D Sc , F N A , F N A Sc , Allahabad

9 Prof Pramod Tandon, Ph D , F N A Sc , Shillong

Members

10 Dr Samir Bhattacharya, Ph D , F N A , F A Sc , F N A Sc , Kolkata

11 Prof Suresh Chandra, D Phil , Grad Brit I R E , F N A Sc , Varanasi

12 Prof Virander Singh Chauhan, Ph D , D Phil (Oxford), F N A , F N A Sc , New Delhi

13 Prof Asis Datta, Ph D , D Sc , F N A , F A Sc , F N A Sc , F T W A S New Delhi

14 Prof Kasturi Datta, Ph D , F N A , F A Sc , F N A Sc , F T W A S , New Delhi

15 Prof Sushanta Dattagupta, Ph D , F N A , F A Sc , F N A Sc , F T W A S , Kolkata

16 Dr Amit Ghosh, Ph D , F N A , F A Sc , F N A Sc , Chandigarh

17 Prof H S Mani, Ph D (Columbia), F A Sc , F N A Sc , Chennai

18 Prof G K Mehta, Ph D , F N A Sc , Allahabad

19 Dr G C Mishra, Ph D , F N A Sc , Pune

20 Dr Ashok Misra, M S (Chem Engg), M S (Polymer Sc), Ph D , F N A Sc ,Mumbai

21 Prof Kambadur Muralidhar, Ph D , F N A , F A Sc , F N A Sc ,Delhi

22 Dr Vijayalakshmi Ravindranath, Ph D ,F N A Sc , F T W A S , Manesar

23 Prof Ajay Kumar Sood, Ph D , F N A , F A Sc , F N A Sc , F T W A S , Bangalore

Special Invitees

1 Prof M G K Menon, Ph D (Bristol), D Sc (h c), F N A , F A Sc , Hon F N A Sc F T W A S F R S Mem Pontifical Acad Sc , New Delhi

2 Dr (Mrs) Manju Sharma, Ph D , F N A A S , F A M I , F I S A B , F N A Sc F T W A S , New Delhi

3 Prof P N Tandon, M S , D Sc(h c), F R C S , F A M S , F N A , F A Sc , F N A Sc , F T W A S Delhi

4 Prof Girjesh Govil, Ph D , F N A , F A Sc , F T W A S , Mumbai

The *Proceedings of the National Academy of Sciences, India*, is published in two Sections Section A (Physical Sciences) and Section B (Biological Sciences) Four parts of each section are published annually (since 1960)

The Editorial Board in its work of examining papers received for publication is assisted, in an honorary capacity by a large number of distinguished scientists The Academy assumes no responsibility for the statements and opinions advanced by the authors The papers must conform strictly to the rules for publication of papers in the *Proceedings* A total 25 reprints is supplied free of cost to the author or authors The authors may ask for a reasonable number of additional reprints at cost price, provided they give prior intimation while returning the proof

Communication regarding contributions for publications in the *Proceedings*, books for review, subscriptions etc should be sent to the Managing Editor, The National Academy of Sciences, India, 5, Lajpatrai Road Allahabad - 211002 (India)

Annual Subscription for both Sections : Rs. 500.00; for each Section Rs 250.00; Single Copy . Rs. 100.00. Foreign Subscription : (a) for one Section : US $100, (b) for both Sections US $200

(Air-Mail charges included in foreign subscription)

Co-Sponsored by C S T U P (Lucknow)

PROCEEDINGS

OF THE

NATIONAL ACADEMY OF SCIENCES, INDIA

2004

VOL LXXIV SECTION–A PART I

Synthesis and characterization of some transition metal complexes of a novel binucleating macrocyclic ligand - 4,14,20,30 – oxo_4 - 8,9,10 ; 24,25,26 - (4-Me phenoxy)$_2$ - [32] - 6,8,11,22,24,27 - hexenato [2-] - 5,6,12,13,21,22,28,29 – N_8 -1,17- S_2

R C. SHARMA*, RITIKA VATS , SHUBHRA SINGH and SANDHYA AGARWAL

Department of Chemistry, Dr. B.R. Ambedkar University, Institute of Basic Sciences, Khandari Road, Agra – 282 002, India

**Address for correspondence : 9, Lata Kunj, Mathura Road, Agra-282002, India.*

Received December 13, 2001, Final Revision February 4, 2003, Accepted September 15, 2003

Abstract

A series of new binuclear macrocyclic complexes of Co (II), Ni (II), Zn (II) and Cd (II) of a novel 32 - membered anionic macrocyclic ligand i e. 4, 14, 20, 30 – oxo_4 - 8, 9, 10 , 24, 25, 26 - (4 - Me phenoxy)$_2$ - [32] - 6, 8, 11, 22, 24, 27 - hexenato [2-] -5, 6, 12, 13, 21, 22, 28, 29 - N_8 -1,17-S_2 has been prepared by condensation of 2,6 – Diformyl - 4 - methylphenol (DFMP) with 3,3' – Thio bis (propionic hydrazide) (TBPH) in presence of metal [M (II)] salts in 1.1 1 ratio at elevated temperature in methanol. The resulting complexes have been characterized by their repeated melting point determination, T L.C., elemental analyses, magnetic studies, molar conductance, IR, NMR and UV-Visible spectral data.

(**Keywords :** binucleating /macrocyclic ligand/transition metal complexes)

Introduction

Transition metal complexes of macrocyclic ligands[1] have great significance as antibiotic[2,3] and fungicidal agents[4]. Macrocycles with schiff base linkage have received great attention during the past few years[5]. Interest has also been focussed on the coordination chemistry of polyamides[6] and polyazamacrocycles[7]. Macrocyclic compounds have also been studied for their use as carriers for ion transport across organic liquid membranes[8]. Polymeric macrocyclic ligands have also been reported as highly selective extractants for metal ions[9,10]. A few binuclear complexes have also been studied for potential catalytic behaviour and investigated for their electronic, magnetic and electrochemical properties[11,12]. This work is carried out as an extension along the above lines with an effort to prepare binuclear transition metal macrocyclic complexes of a new 32-membered anionic macrocyclic ligand **oxo$_4$ [32] hexenato [2-] N_8S_2.**

Materials and Method

All the chemicals used were of A.R. Grade and the solvents were distilled and purified prior to use.

The synthesis of the macrocyclic complexes was carried out in three steps :

1. *Synthesis of 2,6-Diformyl-4-methylphenol [DFMP] :*

It was prepared according to the method given by Gagne *et al.*[13]. [M.P. = 130°C, Yield = 4.5 g (28%)]

2. *Synthesis of 3,3'-Thio bis (propionic hydrazide) [TBPH]* :

It was carried out in two steps :

(a) *Synthesis of Diethyl thiodipropionate [DETDP] :* 3.5 g of thiodipropionic acid was dissolved in 20 ml of absolute alcohol and heated under reflux with 0.3 ml of concentrated H_2SO_4 for 16 hours with small chips of porcelain to prevent bumping. The solution was then cooled and poured into a separating funnel containing 15 ml of water and shaken well. After about 10-15 min., a sharp separation was obtained between the aqueous and ester layers. The lower ester layer was collected and treated with saturated solution of sodium bicarbonate until effervescence ceases. It was finally washed with water several times to obtain the ester.

[B.P. = 148°C, Yield = 1.2 ml (48%)]

(b) *Synthesis of 3,3'- Thio bis (propionic hydrazide) [TBPH] :* 2.3 ml of diethyl thiodipropionate was taken in a round bottom flask, mixed with 0.8 ml of hydrazine hydrate and 20 ml of absolute alcohol and the mixture was heated under reflux for about 4 h. Excess of alcohol was then removed by evaporation. The solution was cooled in a freezing mixture for 24 h The solid obtained was separated, washed and recrystallized from ethyl alcohol. It was dried in vacuum desiccator over anhydrous $CaCl_2$.

[M.P. = 137°C, Yield = 1.1 g (55%)]

3. *Synthesis of Co (II), Ni (II), Zn (II) and Cd (II) binuclear macrocyclic complexes :*

A general procedure was adopted to synthesize the complexes as given :

0.2 ml (1mM) of 3,3'-Thio bis (propionic hydrazide) was taken in 10 ml of methanol and to this 1mM of the metal salt [i.e. 0.25 g of $(CH_3COO)_2Co.4H_2O$ / 0.24g of $(CH_3COO)_2Ni.4H_2O$ / 0.22 g of $(CH_3COO)_2Zn.2H_2O$ / 0.18 g of $CdCl_2$] dissolved in 10 ml of distilled water was added and the resulting solution was heated under reflux with N_2 for 30 min. 0.16 g (1mM) of the synthesized dicarbaldehyde (DFMP) dissolved in 10 ml of methanol was added to the warm mixture of hydrazide and metal salt and together refluxed with stirring under N_2 for 3-4 h. On cooling, the resulting precipitate was collected by centrifugation, washed with cold water, methanol and ether, followed by recrystallization from DMSO. It was dried over anhydrous $CaCl_2$ in vacuum desiccator under reduced pressure. The molar conductance value of the Co-complex is 235 ohm^{-1} cm^2 mol^{-1} and that of the Ni-complex is 245 ohm^{-1} cm^2mol^{-1}. This indicates their electrolytic nature and presence of three ions[14]

Analytical and Physical Measurements : The purity of the complexes was confirmed by running their T.L.C. for single spot on silica gel-G. Carbon, Hydrogen and Nitrogen analyses were carried out on Carlo Erba Micro Analyser (Model-1106) and Sulphur was estimated as $BaSO_4$ by standard procedure[15] . Co, Ni, Zn and Cd were estimated by decomposing their complexes with 5 ml of 1:1 mixture of concentrated HNO_3 and concentrated H_2SO_4 and precipitating them as their pyridine complexes[16]. Molecular weights of all the compounds were determined by Cryoscopic method[17]. IR spectra were recorded on a JASCO Spectrometer (Model IR-Report-100) in KBr medium. Conductance measurements in 10^{-3} M DMSO solutions were made using Toshniwal Conductivity Bridge (Model CLO.1.10A) and magnetic susceptibility was determined at room temperature by Gouy's method. ^1H NMR spectral studies were carried out on NMR Brucker AC-300 MHz in $CDCl_3$. The UV-

Visible spectra were recorded on Shimadzu Digital Double Beam Spectrophotometer (Model UV 150-150.02) using DMSO as solvent.

Results and Discussion

The analytical data of the complexes (Table 1) have been found to be quite close to their expected values for the proposed formula. The IR spectra of the dialdehyde (DFMP) reveal >C=O stretching vibration of aromatic aldehyde group[18] approximately about 1715 -1695 cm^{-1} (sharp) and a peak around 3550-3470 cm^{-1} (broad) due to stretching vibrations of phenolic group. Stretching C-H of aldehyde[19] is obtained at 2880 cm^{-1} (weak) and a sharp peak of C-CH_3 out of plane is obtained at 2972-2953 cm^{-1}. A weak band is obtained about 3010 cm^{-1} due to C-H stretching vibrations of aromatic ring. The IR spectra of the dihydrazide (TBPH) reveal bands around 3290 cm^{-1}, 1600 cm^{-1} and 3210 cm^{-1} which may be attributed to stretching, bending vibrations of primary aromatic amine (-NH_2) and stretching vibrations of secondary amine (-NH-) respectively[20]. A band corresponding to >C=O stretching vibrations is observed at about 1710 cm^{-1}. N-N stretching vibration is also observed at 1050 cm^{-1} and a C-S aliphatic at 645 cm^{-1} respectively. The IR spectra of the metal complexes show a new band in the region of 1640-1630 cm^{-1} due to stretching vibrations of azomethine (>C=N-) group[21] which shifts to the negative side indicating coordination of ligand to metal through nitrogen. The band due to phenolic group disappears indicating bonding of OH group to metal ion through its deprotonation. The coordination through sulphur, nitrogen and oxygen atoms is confirmed by the occurrence of new bands in the regions of 345-330 cm^{-1}, 485-465 cm^{-1} and 570-550 cm^{-1} respectively[22]. ^1H NMR data ($CDCl_3$) δ of the synthesized dicarbaldehyde (DFMP) is observed at 2.2 (3H, s, Me), 7.8 (2H, m, Ar)[23], 10.2 (2H, s, aldehydic)[24] and 11.4 (1H, s, phenolic). The dihydrazide (TBPH) shows δ values at 3.7 (8H, m, -CH_2-), 3.9 (4H, brs, -NH_2) and at 9.1 (2H, brs, -NH-)[25]. The NMR data of the complexes reveals new δ values at 3.1 - 3.3 (6H, m, -CH_3COO^-)[26], 5.0 - 5.2 (4H, s, H_2O) and at 8.1- 8.2 (4H, s, azomethine-H)[27] showing the condensation of DFMP with TBPH which is also indicated by disappearance of δ values of protons of aldehyde and primary amino group. Deprotonation of phenolic OH is also confirmed by the absence of its δ value in the NMR data of the complexes. The UV/VIS transitions of the Co-complex at 8,250 cm^{-1}, 15,855 cm^{-1} and 20,405 cm^{-1} correspond to $^4T_{1g} \rightarrow {}^4T_{2g}$, $^4T_{1g} \rightarrow {}^4A_{2g}$ and $^4T_{1g} \rightarrow {}^4T_{1g}$ (P) respectively, indicating octahedral geometry[28] around central Co - atoms which is also supported by its effective magnetic moment value at 4.75 B.M.[29]. The Ni-complex shows UV/VIS transitions at 10,735 cm^{-1}, 16,410 cm^{-1} and 27,000 cm^{-1} corresponding to $^3A_{2g} \rightarrow {}^3T_{2g}$, $^3A_{2g} \rightarrow {}^3T_{1g}$ and $^3A_{2g} \rightarrow {}^3T_{1g}$ (P)

Table 1– Physical and analytical data

S.l. No.	Name of compound	Molecular Formula	Colour	M P. (°C)	% Analysis Found / (Calculated)					Molecular Weight F/(C)
					C	H	N	S	M	
1.	DFMP	C_9H6O_3	yellow	130	66.11	5.28	–	–	–	176
					(65.90)	(4.80)	–	–	–	(164)
2.	TBPH	$C_{16}H_{14}N_4SO_2$	white	138	35.18	7 04	26.78	1502		219
						(34 95)	(6 79)	(27 18)	(15 53)	(206)
3.	[(CO^{2+})$_2${OXO_4[32] exenato(2-) N_8tS_2}]$^{2+}$ (CH_3COO^-)$_2$. $2H_2O$	$CO_2(C_{34}H_{44}N_8S_20_{12})$	yellowish green	310	43 84 (43 50)	4 99 (4 69)	11 34 (11 94)	611 (6 82)	11 02 (1256)'	949 08 (937 86)
4	[(Ni^{2+})$_2${oxo_4[32] hexenato(2-) N_8S_2}]$^{2+}$ (CH_3COO^-)$_2$ $2H_2O$	$Ni_2(C_{34}H_{44}N_8S_2O^{12})$	bright mustard	330	43 90 (43 52)	4 94 (4 69)	11 26 (11 95)	6 22 (6 83)	11 12 (12 52)	948 08 (937 38)
5.	[(Zn^{2+})$_2${oxo_4[32] hexenato(2-)N_8S_2}]$^{2+}$ (CH_3COO^-)$_2$.$2H_2O$	$Zn_2C_{34}H_{44}N_8S_2O_{12}$)	canary yellow	300	43.16 (42 91)	4 98 (4 63)	11.12 (11 78)	6.10 (6 73)	12.48 (13 7S)	961.20 (950 78)
6.	[(Cd^{2+})$_2${oxo_4[32] hexenato(2-)N_8S_2}]$^{2-}$ (CI-)$_2$. $2H_2O$	$Cd_2(C_{30}H_{38}N_8S_2O_8Cl_2)$	deep yellow	290	36.48 (36.08)	4 16 (3 81)	10 74 (11 22)	5 56 (6 41)	21 19 (22 S3)	1010 24 (997.84)

respectively, suggesting octahedral geometry[30] which is also confirmed by its effective magnetic moment value at 1.95 B.M. This value is less than normal probably due to antiferromagnetic interaction between the two Ni-atoms[31]. The 10 Dq and β values for Co complex are 7605 cm^{-1} and 767 cm^{-1} respectively and for the Ni complex are 10,735 cm^{-1} and 747 cm^{-1} respectively. The proposed structure of the macrocyclic complex is as under :

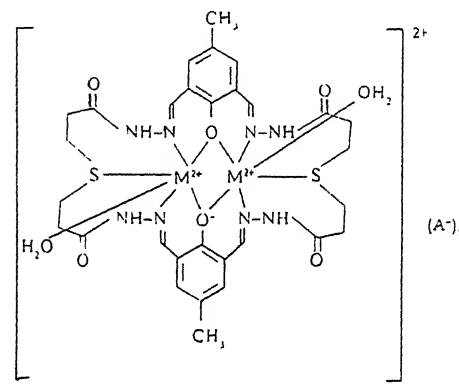

M = Co, Ni, Zn and Cd, A = CH_3COO / Cl

References

1. Sharma, R C & Johari, R B (1987) *J Indian Chem Soc* **125** : 12
2. Singh, N K , Agarwal, Namita & Agarwal, R C (1986) *Acta Chem Hung* **121** 3.
3. Parashar, R K & Sharma, R C (1987) *J Inorg Biochem* **28** 1
4 Farrow, W M , Calvin, H & Schieler, F W (1954) *J Am Phar Ass* **13** · 370.
5. Jaeger, E G (1986) *Zh Chem Ger* **26** 2
6. Singh, R.V., Saxena, C & Fahmi, N (2000) *Synth React Inorg Met Org Chem* **30** 129
7 Goldberg, D.P (1998) *Inorg Chem* **37** . 2873.
8 Ameerunisha, S & Zacharias, P S (1995) *Polyhedron* **14** 2319.
9. Dale, J. (1980) *Isr J Chem* **20** 3
10 Singh, R., Bhattacharya, A , Sharma, Mamta, Bhatt, D & Rekha (2001) *J Indian Chem Soc* **78** 152
11 Maya, E M. (2000) *J Org. Chem* **65** · 823.
12. Bellec, N (2000) *J Org Chem* **65** : 1774.

13 Gagne, R R , Spiro, C L , Smith, T J., Hainann, C A , Thies, W R & Shiemke,A K (1981) *J Am Chem Soc* **103** 4073

14 Mukherjee, G N & Sarkar, S (1994) *J Indian Chem Soc* **71** 45

15 Vogel, A I (1964) *The Text Book of Quantitative Inorganic Analysis*, Green and Co. Ltd , London

16 Trendwell, F P (1968) *Analytical Chemistry*, John Wiley and Sons, London

17 Dean, J A (1978) *Lange's Hand Book of Chemistry*, 12th Ed , McGraw Hill International Editions, p 801

18 Mathis, F (1953) *Bull Chem Soc* **9D** 22

19 Er-Van, T (1965) *J Chem Soc* 5775

20 Fujii, K & Nakao, K (1982) *Synthesis* 456

21 Pang, S M , Gordon, G C & Goedkar, V L (1978) *Inorg Chem* **17** 119

22 Koracie, J E (1967) *Spectrochim Acta* **23A** . 183

23 Shakir, M & Varkey, S P (1994) *Polyhedron* **13** 941

24 Jayaram, B & Mayanna, S M (1983) *Tetrahedron* **39** 2271

25 Girish, S.R & Mahale, B V (1991) *Trans Met Chem* **16** 435

26 Spanel, L & Anderson, M A (1991) *J. Am Chem Soc* **113** 2826

27 Shakir, M , Varkey, S P & Kumar, D (1994) *Synth React Inorg Met Org Chem* **24** · 941

28 Pancholi, H B & Patel, M M. (1998) *J Indian Chem Soc* **75** 86

29 Martin, L Y. (1977) *J Am Chem. Soc* **99** 2968.

30 Panda, A K (1994) *J Indian Chem Soc* **71** 89

31 Sacconi, L (1972) *Coord Chem Rev* **8** 351

PROC NAT ACAD. SCI INDIA, 74 (A), I, 2004

Microdetermination of cerium(III) using 6-chloro-3 - hydroxy - 2 - (2' - thienyl) - 4*H*-chromen - 4 - one

AMITA GARG and L.R. KAKKAR*

**Department of Chemistry, Kurukshetra University, Kurukshetra -1361 19(Haryana), India*

Received June 25, 2002, Revised March 4, 2003, Accepted September 2, 2003

Abstract

A simple and rapid method for the direct spectrophotometric determination of trace amounts of cerium(III) has been worked out using 6-chloro-3-hydroxy-2-(2' -thienyl)-4*H*-chromen-4-one (CHTC) as a complexing agent whose λ_{max} lies at 425nm The method obeys Beer's law in the range 0-2 5 μg Ce ml^{-1} having respective molar absorptivity and Sandell's sensitivity value of 2 03 x 10^4 1 mol^{-1} cm^{-1} and 0 0066 μg cm^{-2}

(Keywords: cerium(III)/spectrophotometry/ CHTC)

Introduction

For the past few years, chromones[1-5] have been frequently employed for the microdetermination of several metal ions which are of much analytical interest. Amongst them, V(III)[6], V(V)[7-10], Nb(V)[8-11], Mo(VI)[12-13], Zr(IV)[14], MO(V)[15] deserve special mention. However, as far as use of chromones and its derivatives in respect of cerium is concerned, the element has not received due attention and thus, needs further study with a view to explore its behaviour towards developing a spectrophotometric method for the trace determination of cerium using (CHTC) as a complexing agent in presence of diphenylamine, with the following details.

Materials and Method

A stock solution of cerium(III),1 mg ml^{-1}, was prepared by dissolving an accurately weighed amount of $Ce(NO_3)_3.6H_2O$ in deionized water. Lower concentrations of the metal ion at the μg ml^{-1} level were obtained by suitable dilutions.

Solutions of other metal ions of appropriate concentration were prepared by dissolving their commonly available salts (AR.) in water or dilute acids.

A 0.1 % (W IV) solution of diphenylamine was prepared in ethanol afresh daily

A 0.01% (W/V) solution of 6-chloro-3-hydroxy-2-(2' -thienyl)-4H-chromen-4-one(CHTC) was prepared[16] in acetone.

For absorbance measurements, a UV -visible spectrophotometer (Shimadzu-UV – 140-02) is used

Procedure

To a sample solution containing 20 μg Ce(III) in a 10 ml measuring flask, add 2ml 0.1% diphenylamine, 0.6 ml 0.01% CHTC and enough deionized water to make up the volume upto the mark. The absorbance of the yellow coloured species is measured at 425 nm against a similarly prepared reagent blank and cerium content is determined from the standard curve drawn by plotting absorbance values corresponding to varying trace amounts of cerium in accordance with the proposed procedure.

Results and Discussion

It has been observed that Ce(III) reacts with CHTC forming a yellow coloured complex in presence of diphenylamine, whose absorption maximum lies at 425 nm. The absorbance measurements are effected in the aqueous phase as the resulting complex is not extractable in any of the commonly available organic solvents.

The influence of variation of temperature, diphenylamine and CHTC on the formation and absorbance of the complex is shown in Table 1. It is evident from the data that for 20 μg Ce, 1.2-2.5 ml of 0.1 % diphenylamine and 0.45-0.7 ml of 0.01 % CHTC in 10 ml final aqueous volume at room temperature are the optimum conditions for the formation of the complex with λmax at 425nm.

Effect of diverse ions

The presence of anion such as sulphate, chloride, nitrate, thiourea, bromide, iodide, nitrite, acetate, (10 mg each); phosphate (1 mg); citrate (0.5 mg); tartrate,

carbonate, (0 1 mg each); in 10 ml aqueous solution containing 20 μg cerium, does not have any effect on the absorbance of the complex and are, therefore, termed as non-interfering. EDTA, fluoride, oxalate, sulphosalicylic acid, interfere. Amongst the cations, in a final 10 ml aqueous volume, As(III), Ce(IV), 1 mg each; Mn(II), Sb(III), Se(IV), Os(VIII), 0.5 mg each; Bi(III), U(VI), Th(IV), Cr(VI), Pt(IV), Nd(III), Pr(III), Sm(III), La(III), 0.1 mg each; Ir(III), Au(III), Re(VII), Pd(II), Zr(IV), Ru(III), Ti(IV), W(VI), Tb(III), Dy(III), Gd(III), Eu(III), 0.01 mg each; Co(II), Ni(II), Ta(V), V(V), 0 005 mg each; Cu(II), Y(III), Ho(III), 0.001 mg each, are not found to show any absorbance under the conditions of the procedure.

Table 1– Effect of various parameters on the absorbance of the cerium complex

1	Temperature(°c)[a]	27*	30	35	40	45	50	60
	Absorbance	0 290	0 290	0 280	0.270	0 260	0 250	0.230
2	Diphenylamine, (ml)[b]	00	0 5	1 0	1 2-2.5	2 6	3.0	5.0
	(0 1 % in ethanol)							
	Absorbance	0 180	0.220	0 270	0.290	0 285	0270	0.120
3	CHTC, (ml)[c]	00	0 3	0 4	0 45-0 7	0 8	0.9	1.0
	(0 01 % in acetone)							
	Absorbance	0 000	0 190	0.270	0 290	0 275	0 250	0.200

* Room Temperature

Experimental Conditions·

(a) Ce(III = 20 μg, diphenylamine, 0.1 %=2ml, CHTC, 0 01 %=0 6ml, temperature = variable, λ_{max} = 425nm

(b) Ce(III) = 20 μg, diphenylamine, 0 1% = variable, CHIC, 0.01% = 0.6ml, λ_{max} = 425nm, at room temperature.

(c) Ce(III) = 20 μg, diphenylamine, 0 1% = 2ml, CHTC, 0.01% = variable, λ_{max} = 425nm, at room temperature.

Spectral studies

The absorption maximum of the Ce(III)-CHTC complex lies at 425 nm where the blank prepared in an analogous manner has the minimum absorbance value. Beer's

law is obeyed in the range 0-2.5 μg Ce ml^{-1} and thereafter, it starts deviating from linearity. The optimum concentration range that can be measured accurately, as evaluated from Ringbom plot, is 1-2.2 ppm of cerium. Molar absorptivity and sandell's sensitivity of the complex are 2.03×10^4 $1mol^{-1}$ cm^{-1} and 0.0066μg Ce cm^{-2}, respectively.

Stoichiometry of the complex

Equimolar solutions of cerium and CHTC reagent (0.0005 M) are employed to determine the metal to ligand ratio in the complex by Job's method of continuous variations as modified by Vosburgh and Cooper. The absorbance values are measured at two different wavelengths namely, 425 and 445 nm. The curves obtained are indicative of 1:2 stoichiometry which is ascertained by mole ratio method as well. The probable structure of the complex is as under.

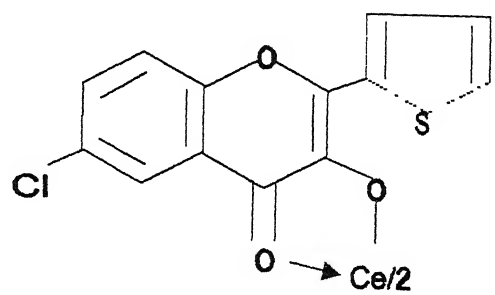

Conclusion

The proposed spectrophotometric method for the determination of cerium is simple, rapid, quite sensitive and free from the interference of a large number of metal ions. The validity of the method is tested by analyzing different samples of varying composition and also that of Australian monazite (Table 2). The result obtained are quite compatible with the amount of metal ion initially added to the sample and are too found to be reproducible. The method compares favorably with the existing methods[17-21] in respect of molar absorptivity and selectivity.

Table 2– Analysis of different samples by the proposed method

S No	Composition of the sample		Ce(III)
	Matrix[a]	Ce(III) added μg	Found μg
1	Mn^{II}(0 5)	5	5 2
2	AS^{III}(0 5)	10	10
3	La^{III}(0 01)	15	15
4	Sb^{III}(0 1), Bi^{III}(0 01)	20	21
5	Ce^{IV}(0 5), As^{III}(0 5)	15	15
6	Ti^{IV}(0 01), W^{VI}(0 01)	10	10 3
7	Os^{VIII}(0.1), Pt^{IV}(0 01), Cr^{VI}(0 0l)	20	21
8	Mn^{III} (0 1), Ce^{IV} (0 1), Se^{IV}(0 1)	5	5 2
9	Nd^{III}(0 01), Pr^{III}(0 01), La^{III}(0 01)	13	12.6
10	As^{III}(0.5), Mn^{II}(0.5), Ce^{IV}(0 5)	17	17
11*	La^{III}(0.05),Th^{IV}(0 01), Pr^{III}(0 012), Sm^{III}(0 01), Nd^{III}(0 045)	15	15 4
12*	La^{III}(O.04), Th^{IV} (0.005), pr^{III} (0 01), Nd^{III}(0 036), Sm^{III} (0.003)	20	20 6

* Sample composition corresponding to Australian monazite

(a) Figure in brackets indicates the amount of metal ion in mg

Acknowledgements

Our sincere thanks are due to the UGC, New Delhi for financial assistance to one of the authors (AG) and Kurukshetra University, Kurukshetra for providing laboratory facilities.

Reference

1. Chhakkar, A.K. & Kakkar, LR. (1995) *Fresenius J Anal Chem* **351** : 720

2 Chauhan, R.S & Kakkar, LR (1994) *Chem Anal (Warsaw)* **12** 571

3 Chhakkar, A K & Kakkar, LR (1995) *Mikrochim Acta* **117** 137

4 Katyal M & Parkash, S. (1977) *Talanta* **24** 367

5 Nevskaya EM & Nazarzenko, V A (1972) *Zh Anal Khm* **27** 1699

6 Agnihotri, N , Dass, R & Mehta, J.R (1997) *Chem Anal (Warsaw)* **42** 397

7 Agnihotri, N , Dass, R & Mehta, J R (1998) *J Indian Chem Soc* **75** 514

8 Agnihotri, N , Dass, R & Mehta, J R (1999) *Anal Sci (Japan)* **15** 1261

9 Agnihotri, N , Dass, R & Mehta, J R (2000) *J Indian Chem Soc* **77** 264

10. Agnihotri, N , Dass, R. & Mehta, J R (1999) *J Indian Chem Soc* **76** 420.

11 Dass, R & Mehta, J R (1997) *Annali di chimica* **87** 653.

12 Dass, R. & Mehta, J.R (1994) *Bull Chem Soc Jpn* **67** 999

13 Dass, R & Mehta, J R (1993) *Bull Chem Soc Jpn* **66** 2251

14 Nijhawan, M & Kakkar LR (1999) *Chem Anal (Warsaw),* **44** 7111

15. Dass, R. & Mehta, J R (1994) *Mikrochim Acta* **113** . 37

16 Tirouflet, J & Cheng, P L (1963) *Bull Soc Chim France* **10** 2252.

17 Zhongzun, Xu & Liaornai, Pan (1987) *Gaodeng Xuexiao Huaxue Xuebao* **8** · 876

18 Ruilin, Wu & Liya, Zhu (1990) *Yezin fenxi* **10** 17.

19 Sharma, Subhash C Tyagi, M P & Purohit, D N (1989) *Orient J Chem* **5** 189

20 Zahi, Qing-Zhou (1994) *Talanta* **41** 703.

21 Yoshida, Isav, Yamamoto, Nobuhiro, Sagara, Fumio, Veno, Keihei, Ishii, Daido & Shinkai, Seizi (1991) *Chem Lett* **12** · 2105.

PROC. NAT. ACAD SCI INDIA, 74 (A), I, 2004

Photocatalytic degradation of azur b and fast green with colloidal anthracene in free and immobilized state

MADHU JAIN, CHARU KOTHARI, ANJU JAIN and P.B. PUNJABI

Department of Chemistry, University College of Science, M L. Sukhadia University, Udaipur – 313002, India

Received August 7, 2002, Revised February 14, 2003, Accepted May 6, 2003

Abstract

The photocatalytic degradation of azur b and fast green has been carried out in the presence of colloidal anthracene supported on polythene films The photocatalytic reaction has been studied spectrophotometrically by observing absorbance at different time intervals. The effect of various parameters like pH, concentration of dye, light intensity, amount of semiconductor etc on the reaction rate was observed A tentative mechanism for the bleaching of dyes has been proposed

(Keywords: spectrophotometry/photocatalytic/azur b/fast green/anthracene)

Introduction

Photocatalytic degradation of organophosphorus pesticides using thin film of TiO_2 has been investigated by Mengyne *et al.*[1] Tennakone and Kottegoda[2] carried out photocatalytic mineralization of paraquat dissolved in water by TiO_2 supported on polyethylene and polypropylene films. Matthews[3] observed the photooxidation of organic impurities in water using a thin film of TiO_2, whereas Tennakone *et al.*[4] reported photoextraction of silver from aqueous solution using anthracene colloid. Tennakone *et al.*[5] studied a simultaneous reductive and oxidative photocatalytic nitrogen fixation in hydrous Fe_2O_3 loaded nafion films in aerated water. Tennakone *et al.*[6] reported photocatalytic degradation of organic contaminants in water with TiO_2 supported on polythene films.

A great deal of literature survey reveals that negligible attention has been paid to photocatalytic reactions using anthracene colloid as a photocatalyst. Therefore, in the present work, colloidal anthracene has been used for the photocatalytic degradation of azur b and fast green in free and immobilized state. Immobilization of colloidal

anthracene helped in combating against the problem of suspension of these particles in aqueous solutions.

Materials and Method

0.0305 g of azur b($C_{15}H_{16}ClN_3S$) or 0.0364 g of fast green ($C_{23}H_{25}ClN_2$) were dissolved in 100.0 mL of doubly distilled water so that the concentration of dye solution was 1.0×10^{-3} M. It was used as a stock solution. The optical densities of the dye solutions were recorded with the help of spectrophotometer (systronics model 106) at λ_{max} 610 nm for fast green and λ_{max} 640 nm for azur b. The absorption spectrum for dyes has been shown in Fig. 1. A polychromtic radiation source (200 W tungsten lamp) has been used for radiation throughout the experiment. The intensity of light was measured by solarimeter Surya mapi model (CEL model 01). An effort has been made to use colloidal anthracene as a semiconductor. As it remains in the form of suspension and, it created problem in the correct measurement of optical densities, therefore, to avoid this problem an attempt has been made to prepare colloidal anthracene as seminconductor supported on polythene films by following method. Circular polythene films cleaned were coated with adhesive (insoluble in water) and then colloidal anthracene powder was spread evenly on the surface of polythene films. After air-drying the films were washed with water to release loosely bound particles of colloidal anthracene and dried at room temperature. Collodial anthracene was prepared using glacial acetic acid in place of propionic acid[4]

Structure of the dyes

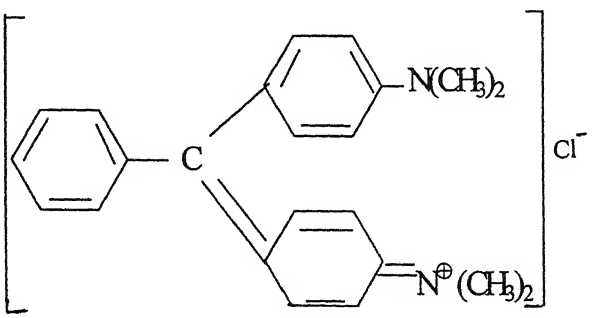

Fast green

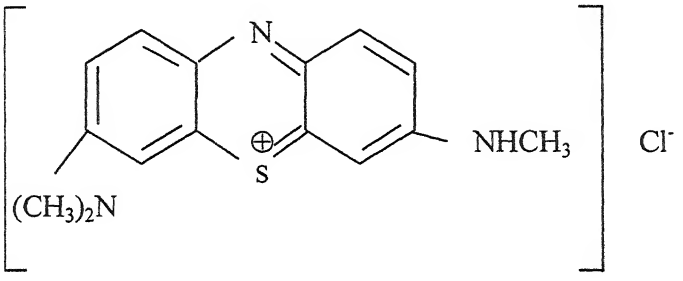

Azur b

Results and Discussion

Effect of pH

The effect of pH on photocatalytic bleaching was investigated (Fig. 2) in the pH range 6.5 to 9.0. It is observed that the rate of photocatalytic bleaching of dyes increase with increase in pH. It was not possible to measure the reaction rate in the pH range below 6.5 because the rate of reaction was very slow. Above 10.0, the rate of reaction is very fast. This can be explained on the basis that on increasing pH, the concentration of OH^- ions will increase in alkaline medium. The semiconductor surface is covered with negatively charged OH ions. The negative charge on the surface of the semiconductor in basic solution will provide a site of attraction for the cationic dye and thus, an increase in the rate of photocatalytic degradation of dyes has been observed

Effect of dye Concentration

The effect of dye concentration on the rate photocatalytic bleaching was investigated (Fig. 3). It has been observed that the rate of photocatalytic degradation increases with an increase in the concentration of the dyes. These changes can be explained on the basis that as the concentration of dyes was increased, more dyes molecules were available for excitation and energy transfer and hence, an increase in the rate. After particular concentration of dye, the rate of photocatalytic degradation was found to decrease with an increase in concentration of the dyes. This may be attributed to the fact that at the higher concentration, dyes will start acting as a filter for the incident light and it will not permit the desired light intensity to reach the semiconducting particles; thus, decreasing the rate of photocatalytic degradation of dyes.

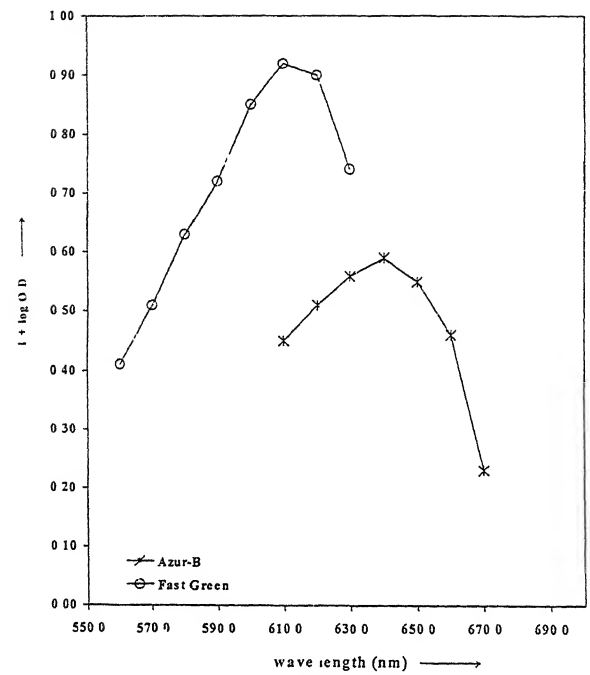

Fig 1– Absorption spectra

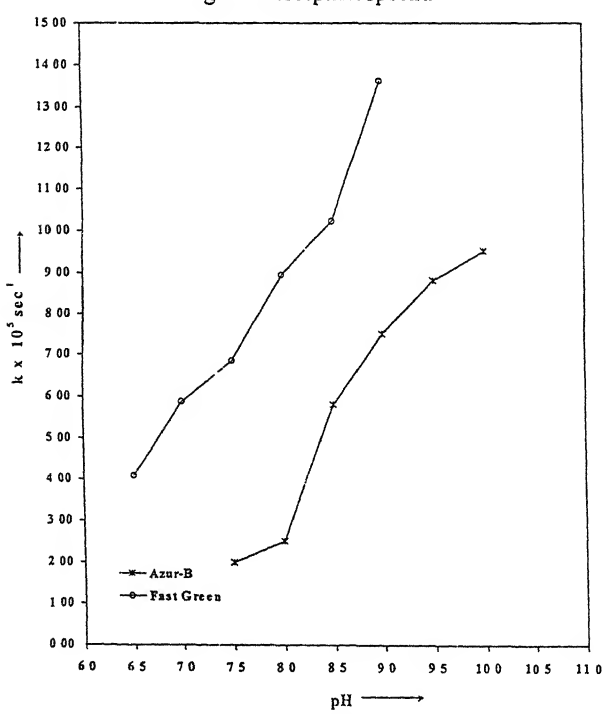

Fig 2– Effect of pH.

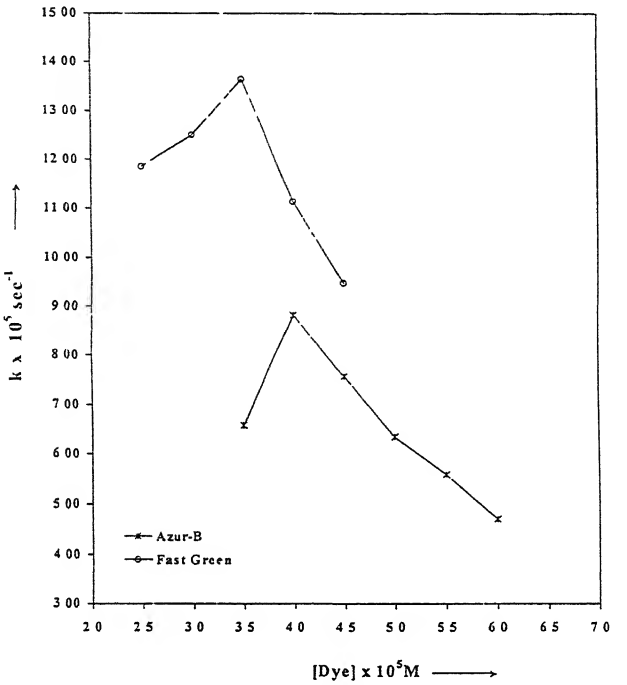

Fig. 3– Effect of dye concentration.

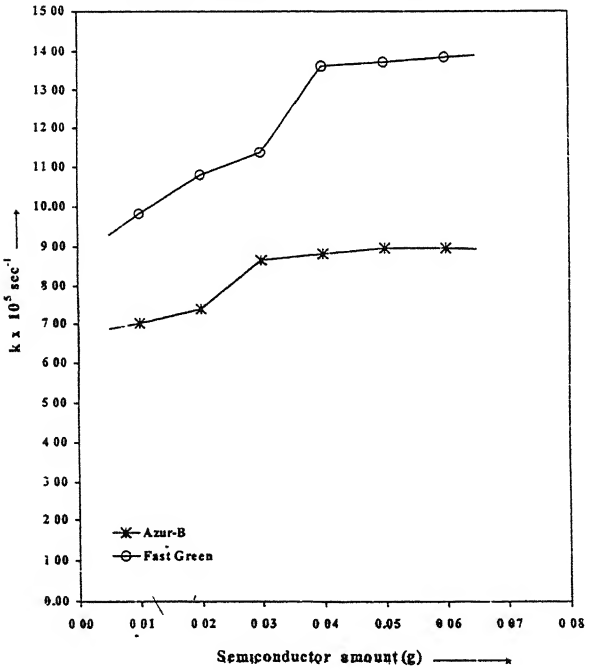

Fig. 4– Effectof amount of semiconductor

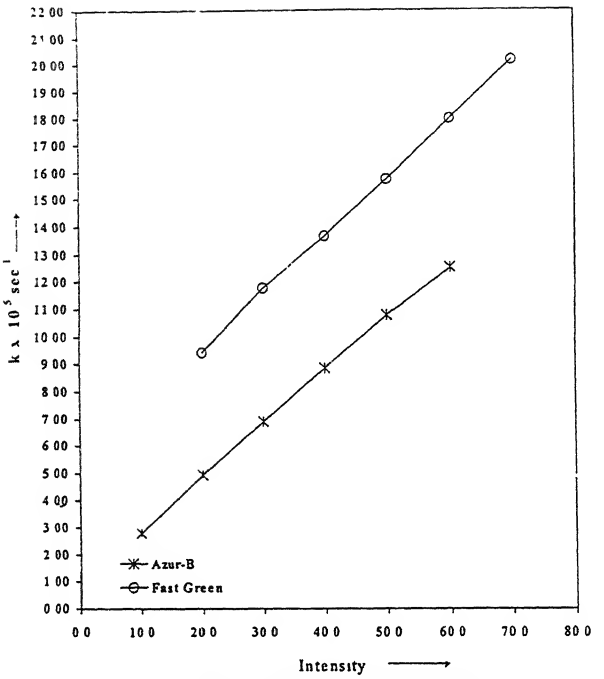

Fig 5– Effect of light intensity.

Effect of amount of semiconductor

The effect of amount of semiconductor on the rate of photocatalytic reaction was also observed (Fig. 4) An increase in the amount of semiconductor increases the rate of photocatalytic reaction up to a certain amount of semiconductor, which is like a saturation point. This can be attributed to the fact that with an increase in the amount of semiconductor, the surface area of the semiconductor will also increase and hence, a corresponding rise in the rate of reaction has been observed. But after a certain limiting amount of semiconductor, if the amount of semiconductor was further increased, and then it will not contribute to an increase in the surface area. On the contrary, it will increase only the thickness of the layer at the polythene film and thus a saturation point like behaviour was observed.

Effect of light intensity

Effect of variation of light intensity on the photocatalytic bleaching of dyes were also investigated (Fig. 5). It has been observed that increase in light intensity increase the rate of reaction. It is because of fact that increase in the light intensity will increase

the number of photons striking per unit area of the semiconductor powder. A linear behaviour between light intensity and rate of reaction was observed.

Mechanism

On the basis of these observation a tentative mechanism for photocatalytic bleaching of azur b and fast green (Dye) may be proposed as :

$$^1Dye_o \xrightarrow{h\nu} {}^1Dye_1$$

$$^1Dye_1 \xrightarrow{ISC} {}^3Dye_1$$

$$\text{Anthracene } (C_{14}H_{10}) \xrightarrow{h\nu} e^-(CB) + h^+(VB)$$

$$^3Dye_1 + h^+(\text{anthracene}) \longrightarrow Dye^+ + \text{anthracene } (e^-)$$

$$\text{anthracene } (e^-) + O_2 \longrightarrow \text{anthracene} + O_2^{\cdot-}$$

$$Dye^+ + OH^- \longrightarrow Dye + OH^\bullet$$

$$Dye + OH^\bullet \longrightarrow \text{Products}$$

Dyes absorb radiations of suitable wavelength and it is excited to its singlet state. Then it undergoes inter system crossing (ISC) to triplet state of the dye. On the other hand, the semiconducting colloidal anthracene[7,8] also utilizes the radiation energy to excite its electron from valence band to the conduction band, thus leaving behind a hole. This hole abstracts an electron from triplet dye and the dye becomes positively charged. The dissolved oxygen of the solution will pull an electron from the conduction band of semiconductor; thus, regenerating the semiconductor. The positively charged molecule of dye will immediately react with hydroxyl ion to form $OH^\bullet$ radicals and these $OH^\bullet$ radicals will oxidize the dye molecule into products, which are colorless.

References

1. Mengyne, Z., Shifu, C. & Yaown, T. (1995) *J Chem Tech and Bio. Tech.* **64** : 339.
2. Tennakone, K. & Kottegoda, I. R. M. (1996) *J Photochem Photobiol* **93A** : 79.

3 Matthews, R W (1987) *J Phys Chem* **91** 3328

4 Tennakone, K , Ketipearachchi, U S , Wijetunga, P A & Vithana, C (1994) *J Photochem Photobiol*, **77A** 265

5 Tennakone, K , Illeperuma, O A , Bandra, J M S , Thaminimulla, C T K & Ketlpearchchi, U S (1991) *J Chem Soc Chem Commun* , 580

6 Tennakone, K , Tilakaratne, C T K & Kottaegoda, I R M (1995) *J Photochem Photobiol* **87A** : 177

7. Meier, H (1974) *Organic semiconductors, dark and photoconductivity organic solids*, Verlag Chemisorb Weinheim,

8 Gutmann, F & Lyons, L F (1967) *Organic semiconductors*, Wiley, New York

PROC NAT ACAD SCI INDIA, 74 (A), I, 2004

Spectrophotometric methods of evaluation of stepwise and overall stability constants of a 1:3 molybdenum - thiolate chelate in chloroform- Comparison with extraction constants and regression analysis

A K CHAKRABARTI

Department of Inorganic and Analytical Chemistry, Jadavpur University, Calcutta 700032, India

Received June 5, 2002, Accepted February 4, 2003

Abstract

Molybdenum (VI) - 2- aminobenzenethiol system have been investigated by solvent extraction. Different photometric methods of evaluation utilizing Harvey - Manning's, Yatsimirskii's and Leden's equations are described, compared and reported in this paper. The values of log k_1, log k_2, log k_3 and log^K obtained by Yatsimirskis equation developed and extended for a 1 3 metal chelate system and based on extrapolation are 2 3, 2 9, 3 4, and 8.6 respectively at 25 ± 1°C The composition was determined and verified by continuous variation and mole ratio methods This was further established and confirmed by solution and solid state analytical methods and elemental analysis of Mo 0 (OH) $(ABT)_3$ Identical log$k$ and log^K values were obtained and agreed well with each other The trend was found to be in the increasing order $k_1 < k_2 < k_3$ The observed sequences on stability constants have been compared and explained by mechanism of formation H-bonding supported the hexagonal dimeric etherate ring structure assigned only in solution and high stability of the oxo-chelate. A statistical regression analysis has been done by standards methods of the equilibria constants. The standard deviations (S D. or s) ± 0 2458, logk_1, 0 04, logk_2, 0 2542, logk_3 and 0 125, log^K and percent relative standard deviations (%RSD = ± 8 19, logk_1, 1 32, logk_2, 8 47, logk_3 and 4 17, log^K for three stepwise and overall stability constants in binary extraction, respectively, have shown high reproducibility. The correlation coefficients (r = 0 8494, n = 3, logk_1; 0.8657, n = 3, logk_1, 0.8983, n = 3, logk_3 and 0 8561, n = 4, logk_{ov} Have also supported excellent precision and reproducibility. The results are very consistent for the stability constants and extraction constant data obtained by spectrometric methods reported in this paper

(Keywords . spectrometric analysis/stability constants/ solvent extraction/ molybdyl chelate/2-aminobenzenethiol/regression analysis/sensitivity)

Introduction

Molybdenum (VI) is important in several different enzymatic, catalytic, redox reactions, wet analysis, spectrometry and biologically active chemical reactive systems[1-5]. MO – S systems are bio-active and active chemical reactive systems to deal with due to redox behaviour[6]. Solvent extractions are the effective procedures to investigate molybdyl – thiolate complexes and certain neutral species. The stepwise formation constants of sulphur chelates are reported quite rarely for future studies and model references. In most of chemical phenomena the thermodynamic equilibrium involving active species and their mechanism of formation are best explained by stability constants. The sequences of their order and trend have very often described and explained mechanistic route, 2-Aminobenzenethiol is a potential biologically active compound. Molybdenum (VI) is also known for its bio-inorganic reactions. Mo (VI) formed stable complexes with sulphur bearing reagents at physiological. pH conditions. The stepwise formation constants of the chelate have been evaluated by a new and novel method utilizing Harvey-Manning's equation based on thermodynamic equilibrium of formation. Photometric methods reported herein are simple, precisely accurate and reproducible. The values obtained were compared to data evaluated by another novel method. The successive formation constants have. also been evaluated by a graphical extrapolation method. The results are in excellent agreement and give the precisional level of high accuracy. The $\log^k$ values differ only by ± 0.1 :in log units on being compared. An increasing stability sequence has been obtained i.e. $k_1 < k_2 < k_3$ in both the methods therein. In this paper a detail report on the methods and a generic discussion and brief review have been dealt with and reported here. The nature of the plots and the related chemistry on complex equilibria are described to focus useful applicability of such model methods.

The aim of the work was to investigate and develop a new method for trace analysis and evaluation of stepwise formation and stability constants by spectrophotometry[9,10]. In this paper, two new methods for molybdenum thiolate system of higher composition has been developed based on Harvey-Manning's and Leden's equation. The results were found to be very much accurate for such systems and they were verified in different metal chelate systems. The extrapolation method with several replicate solutions showed excellent reproducibility. A similar and almost identical numerical values and nature of plots were retained and showed excellent agreement on comparison. A more methodical and detailed description on methods of evaluation and calculations, related equation and their functions with possible explanation for variation with statistical analysis and certainties in their values are described and reported here.

Materials and Method

Instrument. apparatus and reagents

A Hilger – Uvispek SP 600 spectrophotometer was used for all measurements in 1 – cm quartz or glass cells An Elico pH-meter model LI-10 (India) was always used for pH measurements using glass electrode.

Molybdenum(VI) solution

Ammonium heptamolybdate octahydrate was dissolved in water containing a few drops of ammonia and the solution standardized gravimetrically by the 8 - hydroxyquinoline method. A 0.1 mg/ml molybdenum (VI) solution was prepared by dilution of the standard stock solution.

2-Aminobenzenethiol. The reagent is a yellow liquid obtained from Fluka (AR). The reagent was fractionally distilled under reduced pressure. Because the compound is sensitive to atmospheric oxidation giving a disulphide the distillation system was saturated with nitrogen. The product distilling at 88-91°/1 mm of Hg was kept frozen under nitrogen. The pure liquid collected at low pressure is colourless at room temperature. The 2-aminobenzenethiol is a needle shaped white crystalline solid. The pure thiol is stable for indefinite period when kept in the refrigerator.

Chloroform was freed from alcohol by washing with dilute sulphuric acid, dilute ammonia and then twice distilled water. Anhydrous sodium sulphate was used to free organic phase from water.

A 2.084×10^{-2} M reagent was prepared from the stock 2% w/v reagent solution dissolved in pure chloroform always before use.

Procedure

Adjust the pH of the 10 ml aqueous phase containing molybdenum (VI) (1.042 and 2.084×10^{-2} M) equimolar reagent solution and I ml of pure chloroform. Shake the mixture thoroughly for 5 min in a 50-ml separatory funnel, collect the chloroform layer in a 50-ml beaker and dry it over anhydrous sodium sulphate Extract the aqueous phase with further 5-ml portions of chloroform. Transfer the combined extracts quantitatively to a 25-ml volumetric flask and dilute to volume with chloroform. Measure the absorbance at 700nm in 1-cm cells. Construct a calibration curve similarly.

Determination of metal- reagent ratio--Stoichiometry studies

The equi-molar reagent solutions having 1. 042 x 10^{-2} M and 2.084 x 10^{-2} M were prepared by dissolving the purified reagent in alcohol free chloroform. Freshly prepared solutions were always utilized for continuous variation and mole-ratio methods to determine molybdenum (VI) : ABT ratio present in the chelate in chloroform phase. The metal and reagent solutions were continuounsly varied and the green chelate extracted in solvent. The absorbances at 700 nm were plotted against the mole fraction of metal M/M+R in a total volume of 10 or 12 m! In mole-ratio, absorbance obtained with a fixed amount of molybdenum (VI) were plotted against varying amounts of thiol reagent (ABT) added in ml. Here also both solutions are equimolar in concentrations. The composition was determined and verified from the inflexion points. The composition of the chelate (M : R) was determined to be 1:3 measured at 700nm. The nature of reagent effects and mole-ratio plots are reproduced and shown in Fig. 1 (a,b).

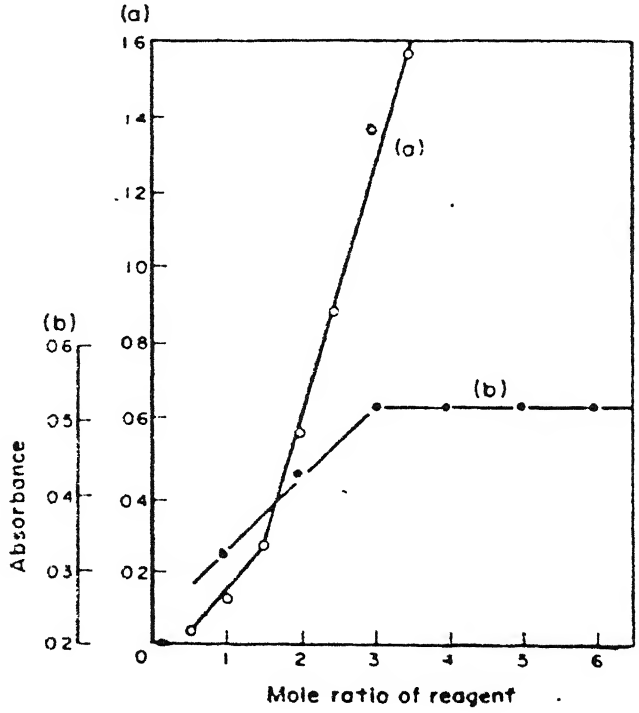

Fig. 1– Mole-ratio plots [a] [M] = [R]= 2.084 x 10^{-2} M Reagent Effect
(b) [M] = 1 402 x 10^{-3}, R = 7.01 x 10^{-2} M

The photometric titration data thus obtained were used to evaluate the stepwise and successive formation constants for neutral species only in chloroform.

Spectrophotometric determination of stepwise formation constants Calculations from Harvey–Manning's equation ·

The degree of dissociation, $\propto$, for any complex system is calculated from generalized equation $\propto = A_m - A_s/A_m$. The complex should possess some dissociating nature with a certain definite value of molar composition[11]. The present system metal-thiolate offers both the properties[12]. It is dissociative in character even in solvent phase and a higher M:R composition of 1.3 is present in the chelate. The equation for thermodynamic equilibria of formation utilized for evaluation of k_1, k_2, k_3, and K are as follows :

$$\begin{array}{lll} MLn & = M + nL & \text{and} \quad \propto = A_m - A_s/A_m \\ (1-\propto)C & \propto C \quad n \propto C & \end{array}$$

Where A_s is absorbance at stoichiometric composition only and A_m is absorbance in presence of large molar excess of reagent. Here, K' = instability constant = $\propto C.(n \propto C)^n/(1-\propto) C$

K = Stability constant = $(1-\propto) C / \propto C.(n \propto C)$

Here, $n = 3$ and $K = k_1k_2k_3$. The stepwise formation or stability constants are calculated considering $\propto$ and its concentration C from above formulations. The stepwise equations are

$K_{11} = 1 - \propto/\propto^2 C$ for a 1: 1 composition, $K_{12} = 1-\propto/4\propto^3 C^2$ for a 1:2 composition and $K_{13} = 1-\propto/27\propto^4 C^3$ for a 1:3 composition of the neutral chelate species. The values of $\propto$ for different species varies with different M:R composition of the said complex. Thus, the thermodynamic constants are different with different $\propto$ values. The $\propto$ values are always raised to the power with increasing metal reagent composition ratio. It is important to note that although the final composition is 1:3 for ML_3 species, k_3 can be calculated using the equation $K = 1- \propto/\propto^2 C$. Because, the composition ML_3 is formed by combination of ML_2 plus L. Thus, n value is unity here and corresponding $\propto$ value is calculated form the stoichiometric absorbencies. Similarly, k_2 is again calculated using the above concept and k_1 is obtained by difference from over-all stability constant for the same complex. The results are given in Table 1.

Table 1– Spectrophotometric determination of stepwise, overall and successive stability constants of molybdenum (VI) complex with 2 - aminobenzenethiol in chloroform solvent at 25 + 1°C Photometric method based on Harvey-Manning's Equation.

A_m	A_r	C	α	$\log k_1$	$\log k_2$	$\log k_3$	$\log K$
0 110	0 005	4 17x10-4M	0 9545	2 07	-	-	-
0 560	0 110	"	0 8035	-	2 86	-	-
1 35	0 560	"	0.5852	-	-	3 46	8 39

Determination of successive and stepwise stability constants. Calculations based on Leden's equation

A novel photometric method has been developed and described based on degree of complex formation function. In this photometric method using graphical extrapolations procedure, the value of φ was evaluated from photometric titration data given by molar ratio studies. The φ is related to successive formation constants β_1, β_2 β_3 and these are inter-related to stepwise constants $\beta_1 = k_1$, $\beta_2 = k_1 k_2$ and $\beta_3 = k_1 k_2 k_3 = K$.

The nature of the plots are shown in Fig. 2. The values of $\log^k$ and $\log^K$ are reported for comparison and the results are given in Table 2.

Absorptiometric determination of extraction constants of molybdyl chelate by modified from of Hiskev-Meloche"s equation :

The auto-synergic equilibria extraction constant of molybdenum(VI) and 2-aminobezenethiol system were determined utilizing Hiskey-Meloche"s equation[15]. The method was modified by replacing the distribution function, D_o, with absorbance term and the graphical plot gives the composition(ML_3) and $\log K_{ex}$. The methods of evaluation of stepwise constants are also briefly mentioned and $\log K_{ex}$ is compared with K_{ov}, obtained by other methods. The extraction equilibria for the thiolate chelate can be written as follows :

i. $M_o0_4(II) + 4H^+ \Leftrightarrow M_oO_2(II) + 2H_2O$

ii. $M_oO_2(II) + HL \Leftrightarrow M_oO_2(OH)L + 2H+$

iii. $M_oO_2(OH)L + HL \Leftrightarrow M_oO_2L_2 + H_2O$

iv. $M_oO_2L_2 \quad H_2L^+ \Leftrightarrow M_oO(OH)L_2^+ + HL \Leftrightarrow M_oO(OH)L_3 + H^+$

where, HL = HABT = 2-aminobenzenethiol (p^A_{SH} = 7.9, p^K_{NH} < 2. The K_{ex} was determined from the following equilibrium ratio relation and represented as follows

$$K_{ex} = [M_oO(OH)L_3]\,[H^+] / [M_oO_z(II)].\,[HL]^3_o = D_o\,[H^+] / [HL]^3_o$$

where, D_o = $[M_o(OH)L_3] / [MoO_2(II)]$ = Distribution or Extraction constant

The results on $\log^K_{1,2,3}$, $\log^K$ and $\log^K_{ex}$ values obtained by photometric methods are given in Table 2. Hence, $\log^K_{ex} = \log^D_o$-pH-3 $\log^{[HL]}_o$ i.e. $\log^D_o$ - pH = 3 $\log^{[HL]}_o$ = $\log\ ^{K_{ex}}$.

Table 2– Molybdenum (VI) - 2 - aminobenzenethiol chelate, Metal = Reagent = 1 042 x 10^{-2} M Metal. Reagent = 1 3 , pH = 2 0 , Solvent = Chloroform, Time for Extraction = 5 min , Metal taken =1 ml of 1 042 x 10^{-2} M Final volume = 25 ml, Total metal conc. = 4.169 x 10^{-5}M Absorbance for metal conc 4 169 x 10^{-5} M = 0.520 . λ_{max} = 700nm

Solu-tion	Total ligand conc , (M/lit.)	Absor-bance	Equilb metal conc , (M/lit)	Conc of metal comple-xed (M/lit)	Equilb ligand conc , (M/lit)	Degree of complex formation function	ψ_1	ψ_2	ψ_3
	(C_L x 10^4)		(x 10^4)	(x10^5)	(x 10^5)	CM/[M]	(x10^{-2})	(x10^{-5})	(x 10^{-8})
1.	4.169	0.025	4.148.	0 2004	4 109	1.005	1 217	1 502	2 682
2	8 338	0 110	4 081	0.8818	8 075	1 021	2 600	2 477	2 572
3	12.507	0.26.0 -	3 961	2 084	11.882	1 052	4 377	3.179	2 340
4	16.676	0 560	3 710	4.489	15 330	1.124	8 087	4.883	2 924
5.	20 845	0.870	3 472	6.974	20 753	1 200	9 636	4.345	1 905
6.	25 014	1.350	3 087	10 820	21 768	1.350	12.770	5 590	2 384
7.	29.183 .	1 550	2 926	12 430	25 454	1.424	16 660	6 310	2 322

Leden's Equation · $\varphi < C_M/M = 1+\beta_1[L]+\beta_2[L]^2+\beta_3[L]^3$, Lim $\psi_1 = (\varphi-1)/[L] = \beta_1 = k_1$ and Lim $\psi_n = (\psi_1-\beta_1)/[L] = \beta_n = k_1\,k_2\,k_3$ (n = 2,3) and $[L] \rightarrow 0$

Intercepts : β_1 =60 x 10^1 β_2 = 40. x 10^4, and β_3 = 2.5 x 10^8

Stability constants: log k_1 =1.79, log k_2 =2.82, log k_3 = 3.90 and $\log^K$ = 8.51

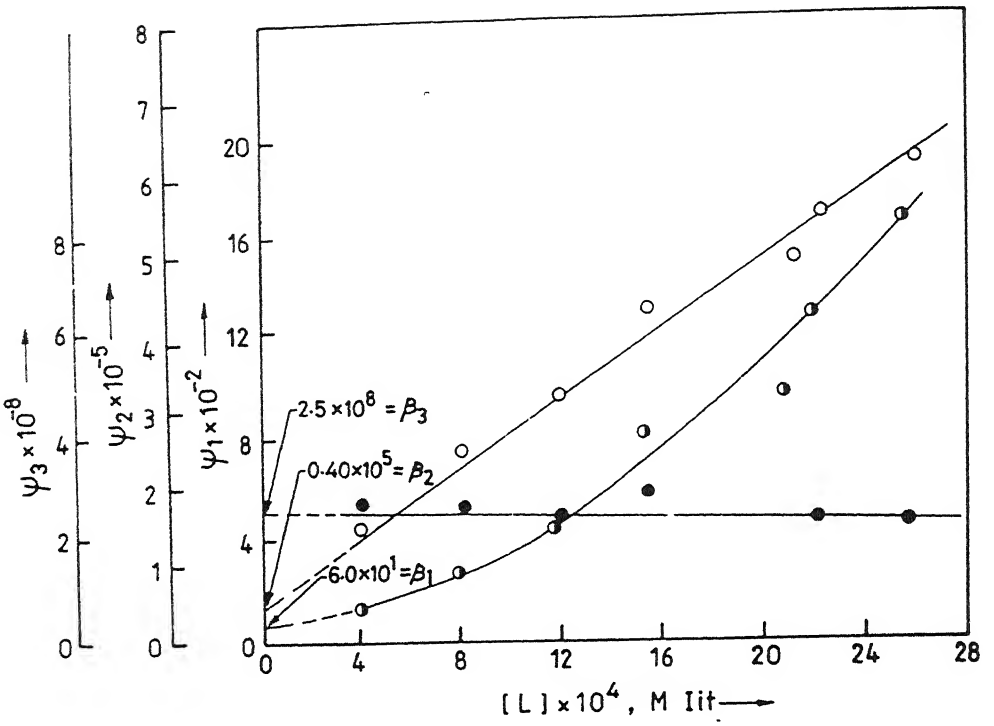

Fig 2–Subsidiary function $\psi_{1,2,3}$ as a function of the free-ligand concentration, [L]

Results and Discussion

Spectra and Composition.

A series of absorbances for the solution mixture containing the complex molybdenum species i.e. ML_1, ML_2, ML_3 were obtained form mole-ratio studies. The complex species are formed with respective formation constants k_1, k_2, k_3. Only these confirmed species are present and either one or all of these species absorbed at 700 nm at the concn. employed because absorbances are additive.

Complex equilibria and dissociation

The system containing above species provides and constitutes complex equilibria. Its formation and dissociation maintains the equilibrium steps. In solutions two

processes are different and solely depends on concn. temperature, nature of ligand, types of reactions and structural chemistry. Just after complex formation the system may dissociates or remain relatively stable. This would be defined by a term extent or degree of dissociation, α. It greatly varies with systems and composition. The concept of formation and dissociation at the same time gives true thermodynamic conditions. α is an important functional parameter. The evaluation of stepwise formation constants is based on this. concept. The instability constant K' is related with K, when K' exists K does also exist. This means with small value of K, a large value of K' results. Thus, when 10% amount of species are formed either 90% amount present has already been dissociated in solution or 90% of actual amount formed dissociates to give a mean value for α. Two phenomena are inter-related because of comparative and competitive reaction sequences. Their order exist to define thermodynamic stability of equilibrium for the metal chelate system. As for example when a 1:1 complex is completely formed then only the 1:2 complex will be formed with excess amount of reagent. It is assumed that concentration C has been utilized. Now only in presence of the reagent in excess to 1:1 ratio, 1:2 complex begins to form, Thus with increased amount of 1:2 species, the amount of 1:1 species gradually decreases and equilibrium is maintained. After certain stage it may so happen that the species dissociates to give 1:1 complex species again increasing its concn. Thus, the equilibrium is maintained and this provides ultimate value of α for 1:2 species. It is essential to point out that there exists some type of over-lapping equilibria due to presence of higher composite species and influenced by nature of ligand, solvent polarity and dielectric constant. The same reasoning is valid for a 1:2 and 1:3 species and actually accounted with observed k and K values obtained by different methods

Degree of dissociation and equilibrium constant

According to Harvey- Manning's method[16] α for any dissociating system can be calculated by the relation, $\alpha = A_m - A_s/A_m$, A_s is absorbance at stoichiometric break point beyond which no other new complex species are formed and maintained the equilibrium set-up condition. Dissociation has been considered here after complete formation of the complex. Thus for a 1:2 species, the equilibrium K i.e. k_2 value can be calculated using the concept that maximum amount of complex is formed corresponding to that at 1:2 composition ratio. Thereafter, increased absorbance is due to new equilibria set-up checked by common ligand anion. The particular 1:2 species is formed from 1:1 species. Hence, equilibrium constant for second step of formation would be given by the following equation : $ML_1 + L \Leftrightarrow ML_2$ and $K = ML_2 / ML_1 \times [L]$ (1:1 species $\Leftrightarrow$ 1:2 species) $K = 1 - \alpha / \alpha^2 C = k_2$ where α is degree of dissociation

for 1:2 species Now, K stands for step II which ultimately depicts k_2 value, Similarly, k_3 value can be calculated using the relation for a mixture of 1:2 and 1:3 complex species.

Influence of solvent and dissociation factors

The maximum absorbance value possible for ML_2 species would be given at stoichiometric M : R ratio. In presence of excess of ligand dissociation will be checked and optimized to give complete thermodynamic condition. It will remain the same because concn. of 1:1 species will also change with excess ligand. But, overall stability constants will be the same. The non-polar solvent served as the carrier phase for such conversion and existences of different neutral species. A definite transition occurs in chloroform from 1:1 to 1.2 species and form 1:2 to 1:3 complex species. Thus, an overlapping equilibria phenomenon is developed for molybdyl thiolate chelate species present in non-aqueous phase. A charged complex is also formed resulting a quick dissociation. There also exists auto synergistic effect with different form of the same ligand. The effect of dielectric constant and photo-decomposition which occurs slowly in chloroform solvent phase accelerates dissociation of H- bond and consequent rapture of M-S bond.

With ABT auto-synergism takes place because ligand is same but existing reagent co-ordinates in different form[17]. The mole ratio plots showing sharp increase in absorbance are included and to show nature of curves sand reproduced here.

Molybdenum (VI) equilibria system :

For Mo (VI) – thiolate system the equilibria can be written in non-aqueous phase as follows: MoO (II) + H^+ + 3 ABT $\Leftrightarrow$ MoO(OH) $(ABT)_3$, a 1:3 neutral species. The dissociation equilibria for ML_3 species is given as

$$ML_3 \underset{\Leftrightarrow}{\overset{\text{Step I}}{\longrightarrow}} ML_2 + L \xrightarrow{\text{Step II}} ML + 2L \xrightarrow{\text{Step III}} M + 3L.$$

The results revealed that the three stepwise formation constants corresponding to reserve equilibrium conditions exists in solvent phase. The sequential values supported its formation mechanism. It is further assumed that all the species co-exists

at a time or in combination at equilibrium. Either all the species absorbs at the same λ_{max} or the final species i e. only 1.3 species absorbs selectively alone at 700mm as maxima Also, this observation is further supported by solid state spectra and solution spectra in chloroform giving same absorbance maxima.

Degree of dissociation and instability constants·

After completion of step I, step II will start till all the species are converted to ML_1 (1: 1) species,. Finally, third step III will result only metal and reagent in solution. The forward reaction is similarly formed till all metal ion is completely complexed by a gradual conversion of 1:1 to 1·2 and then 1:2 to 1:3 complex. Thus, K is inversely proportional to K' and *vice-versa.* After complete formation excess reagent does not change the composition and solely inhibit dissociation. A_m and A_s correspond to the same composition[18]. Here, only amount of complex has increased, but equilibrium constant remains same due to other factor[19]. When $\propto$ varies $\log^k$ values slightly varies for same composition[20]. In exceptional cases overlapping equilibria giving successive formation[21] or dissociation at the same time have indicated variation to a large extent in a metal chelate system. The other spectrophotometric properties and parameters are briefly and concisely summarized in Table-3. The value of $\propto = A_m(1.35) - A_s(.560) / A_m(1.35)$ is 0.5852. The instability constant(K') is obtained by H-M' s equation, $K' = 27 \propto^4 C^3 / 1 - \propto$ for 1 : 3 chelate; C is molar concentration 4.17 x 10^{-4} M. The $\log^K$ is found to be 8.40. The stepwise ,stability constants were determined by H-M method using mole-ratio results and $\log^k$ values were determined to be 2.1, 2.86 and 3.46, respectively. The same amount of metal ion is involved for 1:1, 1:2 and 1:3 complexes. It is presumed that there is no successive formation. After complete formation of 1:1 species, 1:2 species begins to form. The 1:1 species is immediately converted to 1:2 species with excess reagent. Thus, there is minimum dissociation in the medium. Similar is the logic for conversion of 1:2 to 1:3 molybdyl species $K = k_{1,2,3} = 1 - \propto / \propto^2 C$ is valid for each of complex formation equilibrium step. When 1:2 complex is formed from 1:1 complex, A_m for 1:1 species becomes As for 1:2 as the higher composition. Thus, 0.110 is maximum absorbance for 1:1 species after which 1:2 species is formed. So, 0.110 is the stoichiometric absorbance for 1:2 complex and maximum absorbance for 1:2 complex is 0.560. Hence; absorbance becomes maximum for 1:1 ratio and minimum for 1:2 ratio. For final equilibria step, absorbance becomes stoichiometric for 1:2 ratio and minimum for 1:3 ratio in absence of excess reagent. The results on stepwise and overall stability constants i.e. $\log^k$ and $\log^K$ values are given in Table 1. The calculations have been

made on the assumption that complexes are not formed in a stepwise continuous manner and there is a region of stability for each of the complex species. For all the species, only one mole of ligand molecule is bound to each individual species.

Extraction constants by Hiskey-Meloche's equation.

A plot of $\log D_0$ –pH against 3 $\text{Log}^{[HL]}$ gives a straight line with a slope of 3 indicating 1:3 composition of Mo(VI) -thiolate and it is shown in Fig. 4. In the actual plot of modified form of equation, the distribution, D_o, has been replaced by absorbance term $\log A/A_{max}$-A in the modified form of equation. Thus, K_{ex} = $[M_oO(OH)L_3]$ $[H^+]$ / $[M_oO_2(II)]$. $[HL]^3_o$ = $A/A_{max} - A$ x $[H^+]$ / $[HL]^3_o$ (where, HL = HABT, M_o(VI) = Reagent = 2.084 x 10^{-2} M) and $\log {}^{k_{ex}}$ = $\log A/A_{max}$-A –pH+3$\log^{[HL]}_o$ (pH = 2.0); where, A_{max} is absorbance for the complex with excess reagent; A is absorbance with insufficient amount of reagent used in mole-ratio plot and given in Table 4.

A plot of $\log A/A_{max}$-A *vs.* 3 $\text{Log}^{[HL]}_o$ will give a straight line having slope equal to 1:3 (M:L) ratio. The $\log k_{ex}$ is obtained to be 8.30 from the intercept value given through extrapolation. The metal is actually estimated both in aqueous and organic phase. The results have been shown in Table 4. It appeared equivalent to the ratio of abs. terms i.e. A/A_{max} $-A$ and calculated using Beer's law and corresponding absorbance in mole ratio plot. The $\log k_{ex}$ value agrees well with slight variation only in absence of excess reagent. The thermodynamic equilibrium data and $\log k_{ex}$ are given in Table 4.

Stability sequence and statistical regression analysis :

The increasing trend of three stepwise constants ($k_1 < k_2 < k_3$) has been justified and corroborated with other comparative data and competitive data. With 2-aminobenzenethiol reagent the generic trend is in the reverse order. Although they differ but the difference is very close 0.2 in log units. The statistical regression analysis[22] has been carried out with all the equilibrium constants. All the essential parameters to check those values has been calculated to show the excellent range of accuracy and reproducibility[23-25]. The S.D., % RSD, student t-test and correlation coefficients for stability constants are presented in Table-5. The results showed excellent reproducibility within 99 ± 0.5 percent of confidence limits and acceptable precisional level.

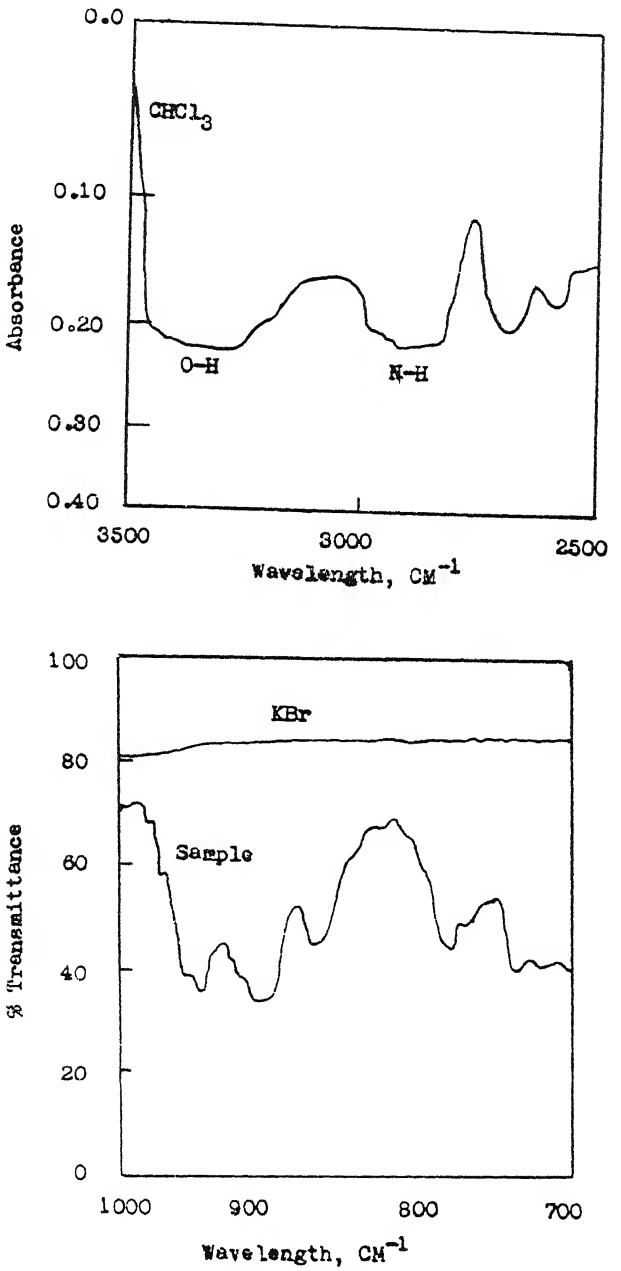

Fig 3– Infrared spectrum of Mo(VI) chelate complex.

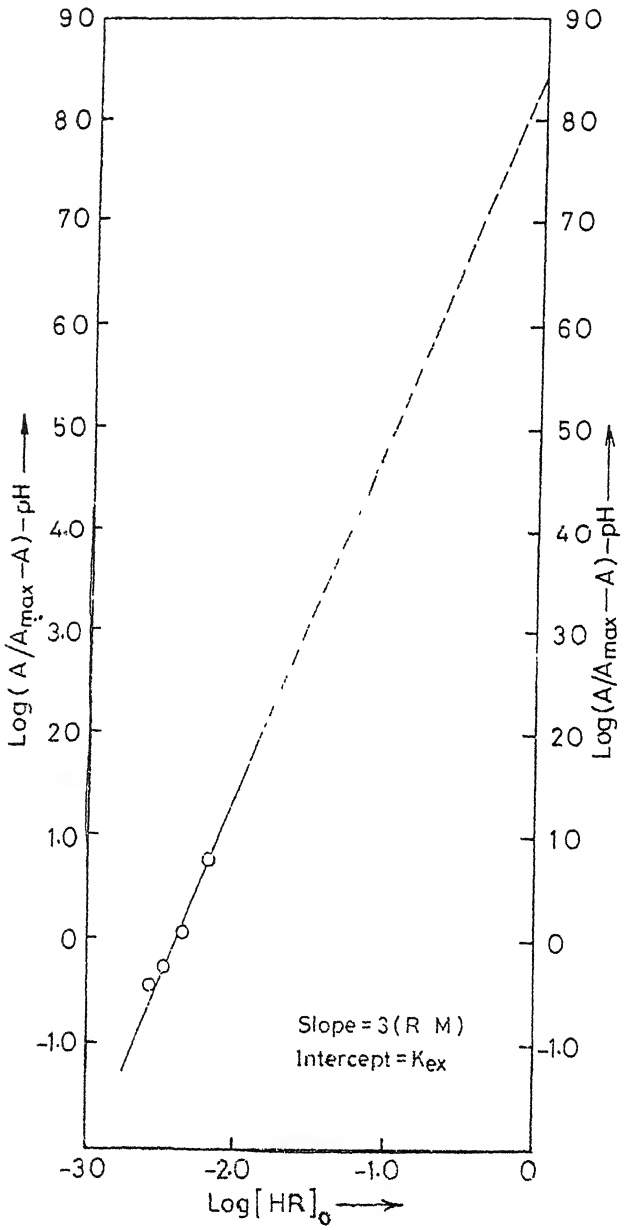

Fig 4–Absorptiometric plot by Hiskey-Meloche's equation.

Table 3– Spectrophotometric and spectral (UV - VIS, IR) parameters of molybdenum (VI)-2-aminobenzenethiol chelate in chloroform

(UV-Visible)	Characteristics	IR Spectra (Nujol / Chloroform)	
Nature	Powder	Str	Frequency
		Mode	Observed, cm^{-1}
Solvent	Chloroform	N-H	3400(s)
Colour	Green		3450(s)
pH-range	1 4 - 2 8 (pH=2 0)	S-H	2550(w)
λ_{max}	700nm		
Beer's law	0 25-10 ppm	N-H	2950(s, $CHCl_3$ H-bonding)
Optimum range	0 5-10 ppm		
Absorptivity	1 25XI0^4 1 $mole^{-1}$ cm^{-1} 7 08X10^4 " (TMA)	O-H	3200-3250 ($CHCl_3$ broad, M-C-H)
Selectivity	Highly selective, 25-fold W tolerated Mo determined in high speed - steel	M-O-H	840 (w, KBr bending)
Sensitivity	0.0075 μg cm^{-2} (7 5ng cm-2) r = 0 8790 (n=7)		870-890(s) 930(sh)
Interferences	Bi, Sn, Re interferes	M-S	Present
H-bond	Inter-and Intramolecular H-bond present in Reagent and chelate		Micro- fine powder Adheres to surface easily
Structure	Hydrogen bonded dimeric structure (orthorhombic)		
Susceptibility	Diamagnetic		
$\log^K$ & $\log^k_{ex}$	8 39(HM), 8 51(Leden), 8 64 (Yatsimirskii), 8.30 (Hiskey-Méloche) r=0 8561 (n=3)		
ΔG°	-11.2K Cal.$mole^{-1}$		
Matrix *a*nalysis	BAS Steel, r = 0.9096 (n=3)		

Table 4– Determination of metal-ligand composition (M L) and extraction constant (K_{ex}) for molybdenum(VI) complex with 2-aminobenzenethiol in chloroform extraction (pH = 2 0) at 25 ± 1°C

Abs	Total ligand Cone , M/L X 10^4	3 log[HL]$_o$	log(A/A_{max}–A)	M L composition	log^K	log$^k_{ex}$
0 025	4 15	-2 91	-1 98			
0 110	8 34	-2 61	-1 91			
0 260	12 51	-2 45	-1 80			
0 560	10 63	-2 34	-1 44	1 3	8 5	8 3
0 870	20 85	-2 21	-0 72			
1 35	25 01	-2 18	-4 70			
1 55	29.18	-2 12				

The influence of solvent dielectric in selective extraction :

The solvent dielectric greatly influences transfer of species through membrane layer and the process of interfacial transfer from aqueous to non-aqueous phase. The volume of extractant has been found to be a prime factor for easy diffusion through membrane layer. The presence of other ions superceeds both the dielectric effect and flow of π -currents and tolerance limits are widely affected. The micro-current generated in the chelate ring nuleus are drifted from the metal complex and tolerance limits are observed to be different with interfering ions. The extraction behaviour with chloroform for recovery of molybdyl thiolate have been found to be of similar nature. Depending upon the extent of such effect the stepwise constants ($k_{1,2,3}$, K) and extraction constant (K_{ex}) did not .differ at all in ultra-trace speciations and the differences in their values are very much negligible in comparison.

Presence of π-rings and effect of micro-current indicated strong influence on the tolerance limits. The increased number of π-rings have increased the chances of in- and out-flow of micro-current giving large variations of tolerance limits. In the process chelation starts with delayed time effect because of greater extent of interaction with ligand environment. When the number of π -rings are evenly poised

on both sides of a chelating group a natural balance of flow π-currents results. Strong chelation and simultaneous bond formation Increased *n*-bonds with greater stabilizing effect minimizes the overlapping criteria. Depending on such extent the k values become close to each other Moreover, with balanced flow of π-current, the reagent and method become more specific in nature. The tolerance limits have increased to a maximum limit The reagent specificity becomes more appropriate for ultra-trace determination of molybdenum with the thiol. The involvement of π-ring and effect of micro-current on tolerance limits in ultra-trace method standardization and determination in matrix samples have been explained

Conclusion

The dissociation and decomposition take place by auto-catalytic reduction and photolytic process in presence of light. For a strong complex or a week dissociating complex. A_m is always greater than A_1 i.e. $A_m > A_{1/2}$. In few examples, $A_m = A_3$ where K for the second step i e. k_2 can easily be calculated by the present method utilizing H-M's equation. In the present chelate a stable M_o = O, M_o - O(H) and M_o - S bonds are formed and possibly controls the three different steps. The H -bond between Mo = O and M_o - 0 - H stabilized the whole molecular system and can well explain the observed reverse trend in stepwise formation constants. Two photometric methods have been tried to evaluate stepwise stability constants for 1:3 (ML_3) complex having the molecular formula $M_oO(OH)(ABT)_3$. In one of the methods the absorbances lower and higher than the stoichiometric break point are involved in extrapolation. Perhaps there is some overlap in the proposed subsidiary functions comprising free-ligand and free-metal. However, the trend is similar and almost provides identical values of stepwise and overall stability constants. Several different species including protonated species i.e. $M_oO_2(ABT)^+$, $M_o0_2(ABT)_2$ and $M_oO(OH)(ABT)_3$ species are present and coexists in solution. The pH (2.0) of aqueous phase controls interfacial distribution process. The solvation of species explained inter-conversion and co-existences of species. All such species absorbs with variable intensity at the same Amax 700 nm. The splitting of energy levels and its average energy values sequentially contributes to the final energy band spectra of the compound molecule. For two of the species the transition is so greatly decreased that the intensity of absorbance of ML_1 and ML_2 becomes too small and it can be neglected. Thiol reagents containing mercapto group (-SH) are not so much susceptible to reduce M_o(VI), a d^o -system. But, a strong complex is formed having a stable M_o - S bond. The compound isolated by mixing and also from chloroform phase are identical and very stable in open air. Molybdenum is potentially involved in several biological functions. Traces of the metal showed

Table 5– Spectrophotometric method of determination of stepwise and over-all stability constants of Mo (VI)-2-aminobenzenethiol chelate in chloroform utilizing different equations at 25 ± 1°C and statistical regression analysis

Method/ Equation	Stepwise stability constants	Overall stability constants	Average value	Standard deviation	Percent relative standard deviation	Student's t-test value	Correlation coefficient
	$Log^{k1,2,3}$	Log^{K}	X, log^{k}, log^{k}	S D. or s	% R S D	t(n=3)	r(n=3)
Harvey-Manning	Log^{k1} - 2 07						
	Log^{k2} - 2 86		Log^{k1} = 2 05	± 0 2458	± 8 19	± 1 61	0 8494
	Log^{k3} - 3.46						
Yatsimirskii	Log^{kl} - 2 28						
	Log^{k2} - 2 90	8 64	Log^{k2} = 2 86	± 0 04	± 1 33	1 73	0 8657
	Log^{k3} - 3.46						
Leden	Log^{k1} - 1 79						
	Log^{k2} - 2.82	8 51	Log^{k3} = 3.60	± 0 2542	± 8 47	2 04	0 8983
	Log^{k3} - 3 90						
			Log^{kov} = 8 51	± 0.125	± 4 17	1 66	0 8561

$t = |(x-\mu)| \sqrt{N}/\text{Std dev.}(s)$, $t = r(n-2)^{1/2}/(1-r^2)^{1/2}$, where, t is Student's t-test values, r = correlation coefficient and the terms t, r have their usual meaning.

complicated equilibria at physiological pH. Its trace determination, equilibria systems and formation constants of different active species formed with sulphur reagents very often furnished different mechanisms in chelate chemistry The stability constants of molybdyl species with active sulphur chain are of interest to elucidate reaction rate and oxidation state in species. 2-Aminobenzenethiol has been found to be a model compound for such novel equilibrium. The quoted references with hydroxy compound showed normal trend for 1:2 complexes e g $k_1 > k_2$. The 1:3 chelates are rarely quoted and the sequence showed rarely any deviation form normal trend. Thermodynamic equilibria of M_o - S bond showing reverse sequence have not been studied thoroughly and reported with any cited system. Auto- protolysis with M_o = 0 chain and autosynergism strongly supports further addition of more ligand giving 1.3 complex The original arrangement is retained, but an hexagonal base plane is formed with N, S in the alternate position giving a highly stable benzene ring structure for the M_o - complex. The oxo- and OH group are placed above and bellow a six-membered ring structure with extra stability in the trans position as shown in Figure. The complex is dissociative in nature due to catalytic reduction and photolysis, solvent dielectric interaction and inter-conversion of the dimer structure to unit octahedral. Presence of excess reagent produced kinetically at a very faster rate giving a sudden increase in absorbance and nullifies all the dissociative effects.

Acknowledgements

The author gratefully acknowledges with thanks the Head, Department of Chemistry for laboratory facilities and the referee towards improvement of the paper. Financial supports from C S.I.R and U.G.C. are gratefully acknowledged.

References

1. Freiser, H (1952) *The Analyst* **77** 830.
2 Dimond, R M (1955) *J Phys Chem* **59** . 710
3 Babko, A.K. (1960) *Russ J Inorg Chem* **64** 822
4 West, R. & Baney, R H (1960) *J Phys Chem* **64** 822
5 Spence, J T (1969) *Coord Chem Rev* **4** 475.
6 Beck, M T. (1970) *Chemistry of Complex Equibria*,. Van Nostrand, London
7 Rossotti, F.J C. & Rossotti, H. (1961) *The determination of stability constant* Mc Graw - Hill,New York
8. Sillen, L.G. & Martell, A.E (1964) *The stability constants*, Part I and Part II, The Chemical Society, London -Reinhold,

9 Tanaka, M & Kojima, I (1975) *AnaL Chim Acta* **75** . 367

10 Yoe, J H & Jones, A L (1944) *Ind Eng Anal Edn* **16** 111

11 Harvey, A E & Manning, D L (1950) *J Amer Chem Soc* **72** 4488

12 Kharsan, R S , Patel, K S & Mishra, R K (1979) *Talanta* **26** 50

13 Chakrabarti, A K & Bag, S P (1976) *Talanta* **23** 736

14 Bag, S P & Chakrabarti, A K (1981) *Indian J Chem* **20A** 482

15 Hiskey, C P. & Meloche, W. (1940) *J Amer Chem Soc* **62** 1565

16 Harvey, A E & Manning, D L (1952) *J Amer Chem Soc* **74** . 4744

17 Chakrabarti, A K (1982) *J Indian Chem Soc* **29** 627

18. Bag, S P , Chakrabarti, A K & Goswami, J P (2000) *Proc Natn Acad Sci , India*, **70A (II)** 159

19 Chakrabarti, A K (2001) *Proc Natn Acad Sci , India*, **71A(II)** 95

20 Chakrabarti, A K (1997) *J Inst Chemists (India)* **69(6)** 181

21 Leden, I (1941) *Z Phys Chem* **188A** 160

22 Levin, R.I & Gubin, D S (1986) *Statistics for management*, 5th, edn , PHI, New Delhi.

23 Christian, G D (1986) *Analytical chemistry*, 4th edn , Wiley, N Y.

24 Youden, W 1 (1951) *Statistical methods for chemists*, Wiley, N Y .

25 Miller, J C & Miller, J N (1992) *Statistics for analytical chemistry*, 2nd edn., Ellis Harwood,

PROC NAT ACAD SCI INDIA, 74 (A), I, 2004

Spectrometric determination of extraction constant and distribution of species by Hiskey–Meloche's equation–Mo(VI)–thiol system

A K CHAKRABARTI

Department of Inorganic and Analytical Chemistry, Jadavpur University, Kolkata – 700 032, India

Received February 19, 1999, Final Revison December 5, 2000, Accepted January 22, 2001

Abstract

A novel spectrometic method of determination of composition and extraction constant (K_{ex}) is reported for Mo(VI) – thiol system The complex formed as a result of auto-synergism is studied by liquid-liquid extraction technique Several neutral species of molybdyl-thiolate chelate is extracted with O-aminobenzenethiol at pH 2.0 in chloroform The distribution of species was calculated based on overall stability constant (Log^{K}=8 3) and its relation with distribution function (D_o) The different neutral species are present which explain the sequence of stepwise stability constants ($k_1<k_2<k_3$) The equilibrium constant parameters are compared and reported here Extraction constant (log K_{ex} = 8 3) is evaluated by a modified form of Hiskey – Meloche's equation A4 to 170 – fold increase in concentration of three species supported and explained the observed trend

(**Keywords** spectrophotometry/extraction constant/ molybdenum/thiol)

Introduction

Molybdenum(VI) is essentially a micro nutrient element present in traces in biochemical system[1]. The stepwise stability constant data would be necessary to give an idea about existence of different species, their nature and bio-chemical activity in traces[2-6]. The extraction constant of a molybdenum(VI) complex is determined utilizing Hiskey-Meloche's equation[7] and distribution ratio function, D_o. The equation has been modified and extended by introducing the distribution function in terms of absorbance, $A/A_{max} - A$. In the present investigation molybdyl-thiolate was extracted from a solution (pH=2.0) in chloroform. The stability constants have been reported earlier[8]. In the present paper, spectrophotometric method of determination of composition and extraction constant of the complex is described. Also, the distribution of different neutral species i.e. ML_1 (1:1), ML_2 (1:2) and ML_3 (1:3) were evaluated by equilibrium conditions. An explanation from structural aspects has supported the

mechanism of formation of species, their stability constants and the trend on formation sequences[9]. The aim of the project is to develop a spectrometric method for molybdyl-thiolate and to determine it's composition, stepwise stability constant, extraction constant and compare them with solvent extraction studies. A 4 to 170 fold increase in complex formation have been observed as a function of free-ligand concentration. Thus stability constant can be utilized to determine the nature of distribution of different absorbing species in organic phase. The extraction constant of a metal-thiol system is not reported earlier in literature. All the results were obtained with high precision.

Materials and Method

The experimental part including the purification of 2-aminobenzenethiol (ABT) has been reported earlier[10].

An aliquot of molybdenum (VI) solution (1.042×10^{-2} M or 2.084×10^{-2} M) was taken in a separatory funnel. The volume of aqueous phase was made 10 ml. pH was adjusted to 2.0. A freshly prepared regent in chloroform was added and the volume of the organic phase was kept at 6 ml. The mixture was shaken thoroughly for 5 min. and allowed to settle. The chloroform layer was collected in a beaker and dried over anhydrous sodium sulphate. The extraction was again repeated for complete extraction with 6 ml portions of choroform. The extracts were transferred to 25 ml flask. The volume was made upto the mark with chloroform. A reagent blank was prepared similarly. The absorbance was measured at 700 mm using 1-cm cell against reagent blank. A calibration curve was constructed similarly.

Determination of composition : The equimolar solutions of metal and reagent ($C_{Mo} = C_{ABT} = 1.042 \times 10^{-2}$ M and 2.084×10^{-2} M) were mixed in complementary mixture of 12 ml volume in continuous variation method. The plot of absorbance against mole fraction gave a composition of 1:3 (Mo: ABT). It was also verified by mole-ratio method. Both studies confirmed the same composition (M:R) for the green chelate.

Determination of extraction constant by Hiskey-Meloche's equation : The equilibria extraction constant and stability constants of the molybdenum(VI) – thiol system were determined by modified form of Hiskey-Meloche's equation and the data were utilized to obtain composition and K_{ex}. Equimolar solutions of metal and reagent o-ABT [Mo (VI) = ABT = 2.084×10^{-2} M] were used to determine the M:R composition ratio in chloroform by the absorptiometic plot and also by continuous

variation and mole-ratio methods as reported earlier. The methods of determination of stepwise constants of neutral chelates were briefly described elsewhere[11-13]. The extraction equilibria for a 1 3 thiolate is written as follows :

$$(i)\ 2\ MoO_2^{2+} + 6H^+ \rightleftharpoons 2\ MoO\ (OH)^{3+} + 2H_2O$$

$$(i)\ 2\ MoO\ (OH)^{3+} + 3HL \rightleftharpoons 2\ MoO\ (OH)\ L_3 + 3H^+$$

The K_{ex} was determined from the following equilibrium ratio relation and represented as follows :

$$K_{ex} = \frac{[MoO\ (OH)\ (L)_3].\ [H^+]}{[MoO\ (OH)^{3+}].\ [HL]^3} = \frac{D_o\ [H^+]}{[HL]^3}$$

Here, Mo(VI) reacts with the reagent to give, 1:1, 1:2 and 1:3 neutral species in chloroform. Three different species are formed and represented by the usual relations : $M + L \rightleftharpoons ML_1$, $ML_1 + L \rightleftharpoons ML_2$ and $ML_2 + L \rightleftharpoons ML_3$. The value of k_3 is evaluated considering n=3 here and it is based on the equation valid for a 1:1 single species having the ML_2 : L as 1:1 ratio. The value of k_1 is calculated by difference from K for the same complex. The results are given and discussed here,

$$Log^{Kex} = Log^{D}{}_o - pH - 3\ Log^{[HL]}{}_0$$

$$i.e.,\ Log^{D}{}_0 - pH = 3\ Log[HL]_o + Log^{Kex}$$

A plot of D_0 – pH against Log $^{[HL]o}$ gives a straight line with a slope 3 indicating 1:3 composition. In actual plot D_0 has been equated and replaced by absorbance term $A/A_{max} - A$ in the equation.

Results and Discussion

Synergistic effect of stepwise formation and stability constant :

The overlapping condition leads to a smooth transition from 1:1 to 1:3 chelate Presence of excess reagent maintained the equilibrium and checked the dissociation of the complex species. With much excess concentrations of the ligand, alternating interactions persist which may result in a slight decrease in absorbance. In absence of interactions there is no such decrease in absorbance. The effect becomes prominent in the continuous variation plot. Protonation of either the ligand N-atom or the 1:2 chelate leads to auto-synergism with the additional ligand molecules and it is facile. In presence in chloroform solvent, it gives rise to some sort of solute-solute interactions. That is why in some mole-ratio plots A_s and A_m values are the same. The excess amount of reagent does not change the composition. A straight line from A_s to A_m becomes parallel to x-axis.

Stability and structures Molybdenum(VI) and ABT are both biologically active. At the physiological pH, their redox reactions furnished few model mechanisms to elucidate the reaction rate and oxidation state in several biological functions. The reagent is supposed to act as a model compound for such novel equilibria phenomenon. The stability constants involving different species at equilibrium showed normal trend. Formation of protonated species and IR spectra confirmed the presence of Mo = O chain, Mo – OH and Mo – S bonds and also H – bond in the thiolate chelate system. All these contributed to a proposed octahedral geometry. The increasing trend, high stability and sequence of stepwise constant values are explained on the basis of intermolecular H-bonding, atuo-protolysis and auto-synergism. The formation of unit octahedral structure and their inter-conversion to dimeric form gave high themal stability both in solid and solution state. Decomposition by auto-catalytic reduction and photolysis by light source may take place in solvent. For weakly dissociating complex $A_{m>>}A_s$. But in almost all examples $A_m = A_s$ or A_m is slightly greater than A_s. However, the stepwise constants can also be evaluated using H-M's equation.

IR spectra and nature of molybdenum chelate : A 1:3 complex, MoO (OH) $(ABT)_3$, is formed when 2% reagent is used. The isolated complex from chloroform and alcoholic solution ($<10^0$C) showed similar absorption spectra and in stretching frequencies in the same region both in KBr pellets and in chloroform phase. A stable Mo = O, Mo-O(H) and Mo-S bonds are formed. An octahedral structure is initially formed and then fused together to give a hexagonal base plane with Mo=O and Mo-OH groups placed trans position. The H-bonding between Mo=O and Mo-OH

stabilised the system. Protonation enhanced the phase transfer during extraction through increased polarisation and % extraction. This leads to a rapid transportation of the species by membrane interface. Based on spectral studies, magnetic susceptibility, TGA studies and IR spectra the present structural configurations are proposed and supported by stability constant data. There is enough evidences from experimental observations to indicate and suggest the proposed structural configuration of molybdy thiolate. This also supported the observed trend and order of stepwise formation constants, $k_1 < k_2 < k_3$.

Composition and extraction constant · Molybdenum : ABT ratio was found to be 1:3 by continuous variation and mole-ratio methods. In the complex the composition was also determined to be 1:3 by absorptiometric plot utilizing Hiskey-Meloche's equation. The extraction constant K_{ex} was obtained from a plot of Log $(A/A_{max} - A)$ – pH *vs.* Log $^{[HL]}{}_o$ to be 8.3 ($\text{Log}^{K\,ex}$) as the intercept (Fig. 1). A simultaneous sequence of distribution as coupled with release of H^+ in presence of large excess of reagent takes place quite readily and extracted in chloroform during extraction. A plot of Log D_0 – pH or Log $(A/A_{max} - A)$ – pH yields a straight line with a slope equal to 3. Thus, the ratio of metal : reagent was obtained to be 1:3 and K_{ex} as the intercept, Log K_{ex} = 8.3. If the complex is highly dissociating in nature Log K_{ex} differs considerably from K_{ov} at equilibrium. Usually, pH value is involved in the plot which gives lower intercept value. The change over value can be explained considering thermodynamic concentration factor in the equilibrium. In most of the chelate complexes K_{ex} differs from K_{ov} at a particular temperature. The results obtained are given in Table 1.

Table 1– Determination of metal-ligand composition (M L) and extraction constants (*K*ex) for molybdenum(VI) complex with 2-aminobenzenethiol in chloroform extraction (pH=2.0) at 25 ± 1°C

Absorbance	Total Ligand C_L, Mole/L x 10^4	3 Log $^{[HL]}$	Log $^{(A/A\max-A)}$	M L Composition	Log^K	Log^{Kex}
0 02	4 15	-2 91	-1.984	1:3	8 3	8 3
0 11	8 34	-2 61	-1 911			
0.26	12 51	-2 45	-1.798			
0 56	10.63	-2 34	-1 44			
0 87	20.85	-2.21	-0 72			
1 35	25 01	-2 18	4 70			
1.55	29.18	-2 12				

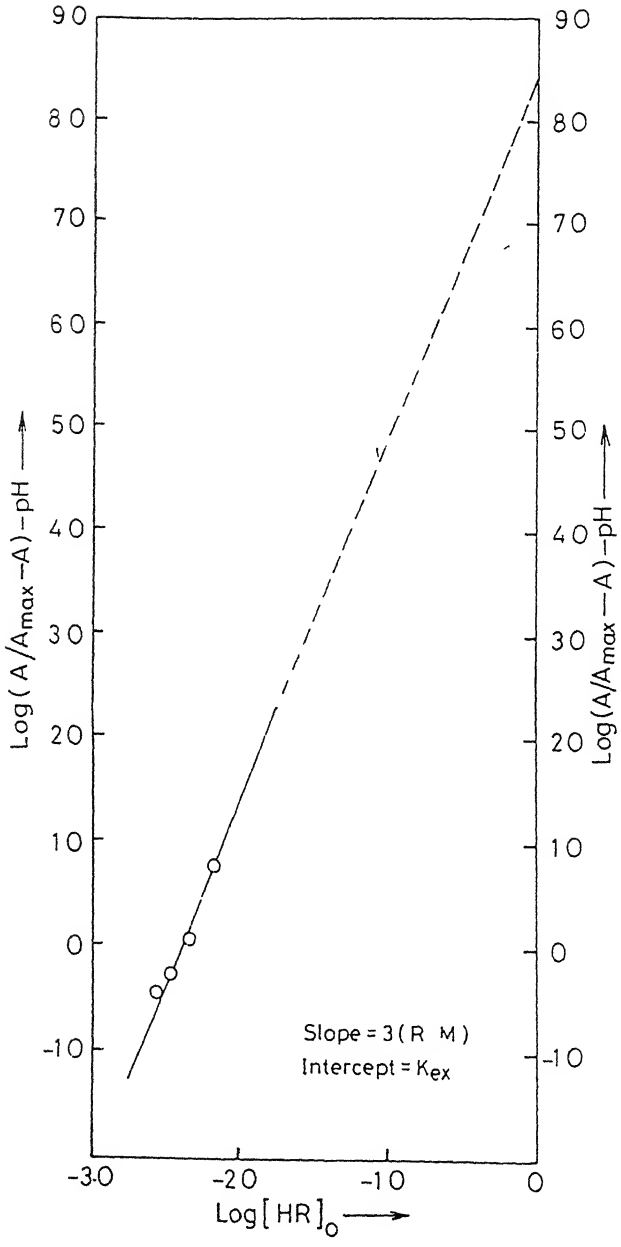

Fig. 1–Absorptiometric plot by Hiskey-Meloche's equation.

The sequence of stability constants and stability factors : The sequence i.e. $k_2 > k_1$, is thus realized and supported by above reasoning. Also, the indentical k_3 value was obtained by three different methods. Again, a reverse order i.e. $k_3 > k_2$ showed still increased stabilizing effects. It is assumed that hydrogen bonding between – OH group and amino N- atom resulted in formation of an ion-pair or associated complex, ML_3, k_3 is slightly increased compared to k_2 since there exists a greater bond strength with highly operative Mo-S bond. There is every possibility that a neutral complex is formed which is extracted in chloroform. Thus, the increased value of k_3 is explained on the assumptions that an orthorhombic structure is formed with three delocalized units attached to central molybdyl ion resulting a neutral complex. Both the species would be extracted in chloroform. The H-bond formation between – OH and Mo=O chain resulted still greater extrastabilizing effect[14]. The chelate molecule is highly stabilized through the formation of a stable benzene like planar base ring structure with H-bonds present in dimeric form. The absorbance increased sharply with excess reagent. Extraction behaviour indicated high dissociative nature of Mo-complex. Third step ligand attachment resulted in increased delocalization and extra stablization by H-bonding of the 1:2 species. Presence of delocalized ring units, rigidity of molecule and H-bonds are sufficient to explain the saturation of coordination no. and the observed stability order. Enough contribution are there to form a hexagonal planar base giving strong conjugated system giving overall stabilization. Pronounced auto-synergism stablizes the molybdyl chelate otherwise formed rapidly with excess reagent supressing dissociation and resulted high thermodynamic stability. Higher stability is due to statistical factor arising from electrostatic bond between two charged species as extractable ion pair in chloroform. This occurred due to stacking interactions by excess reagent in addition to charge neutralisation. Only photo decomposition accelerates dissociation and decomposition in solvent media. H-bonding results in a certain change in species and a drift towards stability sequenc[15].

Structural aspects : The intra-molecular H-bonding increased chelate stability to a great extent. On the other hand, deprotonation of Mo=O chain and a drift in Mo-O-H bond leads to a natural growth of inter-molecular H-bond between M-OH and either ligand N-atom or Mo=O bond. Covalency of 1:2 species is retained, but high ionicity develops. In presence of autosynergism a pressure gradient occurs and finally neutralized by other end groups of S-atom. The outside pressure gradient is created by H-bond and results to stabilize it firmly with another molecule. Also, its formation is enhanced by auto-catalysis showing gradual transition from high covalency to high ionicity and vice cersa.

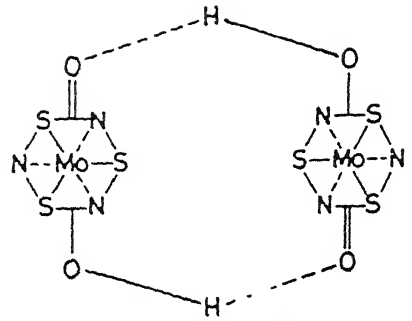

Dimeric structure of Molybdenum (VI) Complex. 8-Coordinated Saturated & H-bonded Chelate complex with 2-aminobenzenethiol.

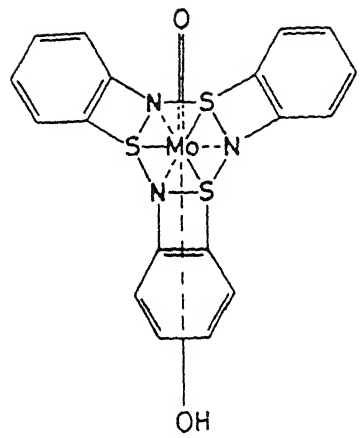

Monomeric structure of Molybdenum (VI) Complex: Octahedral fused ring structure with hexagonal planar base with Mo = O group and M-OH group in transposition.

Fig. 2– Schematic presentation of the proposed structure of the complex.

Table 2– The distribution of 1:1 (ML_1), 1.2 (ML_2) and 1.3 (ML_3) species of molybdyl-thiolate complex as a function of free-ligand concentration, [L]

Abs.	Total Ligand conc., M/Lit x 10^4	Free-ligand conc., M/Lit x 10^4	Conc of 1 1 Species, ML_1 x 10^6, M/L	Conc of 1:2 species, ML_2 x 10^7, M/L	Conc of 1.3 species, ML_3 x 10^4 M/L
0.025	4 15	4 1	21 44	0.658	0 078
0 110	8 35	8.1	41.64	2.552	0 553
0 260	12 51	11.9	59.37	5.293	1.81
0 560	10 63	15.30	71 52	8 198	3 61
0 870	20 85	20.8	90 94	14.17	8 49
1.35	25.01	21 8	85.14	13 91	8.74
1.55	29.18	25 5	94.14	17 99	13 21

Distribution of species as function of ligand concentration · The distribution of different species as a function of free ligand [L] concn. was calculated using the relation : $C_{MLn} = Kn\downarrow X [M]. [L]^n$. It has been found that there is a change in concentration. Thus, there is a 4-fold increase for ML_1 species (21.44 to 94.14 x 10^{-6} M), 27-fold increase for ML_2 species (0.66 to 17.99 x 10^{-7} M) and a 170-fold increase of ML_3 species (0.08 to 13.21 x 10^{-4} M) with added ligand concentration. Thus, species competitively predominates in the solvent phase and contributes to the stability values. Also, this variation and distribution data clearly supports the stability sequence for model metal thiolate chelate. Thus, a consistent results have been obtained form mole-ratio studies[16]. The results are summarized in Table 2. The distribution of species more significantly depends on concentration of proton in distribution medium and dielectric constant of solvent rather than equilibrium constant. The distribution of different neutral chelate species of molybdenum (VI) oxo-chelate can easily be calculated from values of stepwise stability constant and free-ligand concentraction. The free-ligand is calculated from mole-ratio titration and Beer's law absorbance data.

References

1 Spence, J.T. (1969) *Coord, Chem Rev* **4** 475

2. *Metal Ions in Biological Systems* (1973) ed H Sigel, Marcel Decker, New York, Vol 2

3. Gowda, H S., Ramappa, P.G & Nayak, A N., (1979) *Anal Chim Acta* **108** · 277.

4. Ramappa, P.G Gowda, H.S. & Nayak, A N. (1993) *Analyst,* **105** : 663

5 Ramappa, P.G & Revanasiddappa, H D. (1993) "*Biological and Chemical Aspects of Thiazine and Analogs*", Elsevier, Paris.

6. Ramappa, P.G. & Ramachandra, K S (1986) *Curr. Sci* **55** . 34.

7 Hiskey, C.P. & Meloche, V.W. (1940) *J Amer Chem Soc* **62** 1665

8. Chakrabarti, A.K (1997) *J Inst Chemists (India)* **69** · 181

9. Chakrabarti, A K. (1976) *Talanta* **23** 736.

10 Bag, S.P & Chakrabortı, A.K. (1981) *Indian J Chem* **20**A 482.

11. Yoe, J.H. & Jones, A L. (1944) *Ind Eng Chem Anal Ed* **66** 111.

12. Chakrabarti, A.K (1997) *J Inst Chemists (India)* **69** . 177.

13. Harvey, A E & Manning, D.L. (1950) *J Amer Chem. Soc* **72** : 4488.

14. Ballamy, L.J. (1958) "*The infrared spectra of complex molecules*", 2nd Ed , Wiley, New York.

15. Beck, M J. (1970) "*Chemistry of Complex Equilibria*", Van Nostrand, Reinhold, London.

16. Chakrabarti, A.K. (1998) *J. Inst. Chemists (India)* **70** . 81.

PROC. NAT. ACAD. SCI. INDIA, 74 (A), I, 2004

A generalized estimator in econometric methods

R. KARAN SINGH and N. RASTOGI

Department of Statistics, Lucknow University, Lucknow 226 007, India

Received October 27, 2001; Accepted July 12, 2003

Abstract

In econometric methods, linear regression models are widely used, different inference procedures have been developed and their properties are analyzed. Here, we develop a generalized class of estimation procedures which as the special cases, contains ordinary least squares estimator (OLS), restricted least squares estimator, ridge regression estimator and some more available in the literature. This study gives the unified approach to analyze the properties of various particular estimation procedures in regression models.

(Keywords: generalized estimator / generalized bias / variance-covariance matrix)

Introduction

Let the linear regression model be

$$y = X\beta + u \tag{1}$$

where y is an nxl vector of observations on the variable to be explained, X is an nxp full column rank matrix of n observations on p explanatory variables, β is a px 1 vector of regression coefficients and u is an nx 1 vector of disturbances with mean vector 0 and variance - covariance matrix $\sigma^2 I_n$.

The ordinary least squares estimator (OLS) of β is

$$b = (X'X)^{-1} X'Y \tag{2}$$

and, for the exact linear restriction

$$R\beta = r \tag{3}$$

where R is a qxp known matrix with rank q ($<p$) and r is a qxl known vector, the restricted least squares estimator (see Johnston[1]) under the restriction (3) on β is given by

$$b_R = b + (X'X)^{-1} R'[R(X'X)^{-1}R']^{-1} (r - Rb). \quad (4)$$

The ordinary ridge regression (ORR) estimator used as a solution to the problem of multicollinearity (see Hoerl and Kennard[2]) is

$$b^*_{(k)} = [I + k(X'X)^{-1}]^{-1}b \quad (5)$$

where $k(\geq 0)$ is a characterizing scalar to be chosen suitably.

Further, the restricted ridge regression (RRR) estimator by Sarkar[3] is

$$\beta^*(k) = [I + k(X'X)^{-1}]^{-1} b_R \quad (6)$$

where $k(\geq 0)$ is the characterizing scalar and b_R is the restricted least squares estimator for β.

Seeing the forms of the estimators in (2), (4), (5) and (6), we define a generalized estimator b_G of β as

$$b_G = f(b) \quad (7)$$

where, for known W and $f'(\beta)$ being the first order differential coefficient of $f(b)$ with respect to b at the point $b = \beta$, $f(b)$ is a function of b such that

(i) $f(b) = f'(\beta).\ b + W$ and

(ii) $f(\beta) = f'(\beta).\beta + W$

$= E\ [f(b)]$.

It may be mentioned here that $b_G = f(b)$ reduces to

(i) the OLS estimator b with $f'(\beta) = I$ and $W = 0$

(ii) the restricted least squares estimator b_R with

$$f'(\beta) = I - (X'X)^{-1}R'[R(X'X)^{-1}R']^{-1}R$$

and $$W = (X'X)^{-1}R'[R(X'X)^{-1}R']^{-1}r$$

(iii) the ordinary ridge regression (ORR) estimator with

$$f'(\beta) = [I + k(X'X)^{-1}]^{-1} \text{ and } W = 0$$

and

(iv) the restricted ridge regression (RRR) estimator with

$$f'(\beta) = [I + k(X'X)^{-1}]^{-1}\{I - (X'X)^{-1}R'[R(X'X)^{-1}R']R\} \text{ and}$$

$$W = [I + k(X'X)^{-1}]^{-1}(X'X)^{-1}R'[R(X'X)^{-1}R']^{-1}r.$$

Bias and Mean Square Error Matrix of b_G

We have

$$E[f(b)] = f'(\beta)\beta + W$$

so that bias vector of $f(b)$ is

$$E[f(b)] - \beta = f'(\beta)\beta - I\beta + W$$

Or $$\text{Bias}(b_G) = [f'(\beta) - I]\beta + W \qquad (8)$$

$$= B$$

The variance - covariance matrix of b_G is

$$V(b_G) = E[f(b) - E\{f(b)\}][f(b) - E\{f(b)\}]'$$

$$= E[f(b) - \{f'(\beta)\beta + W\}][f(b) - \{f'(\beta)\beta + W\}]'$$

$$= E[f'(\beta).b + W - f'(\beta)\beta - W][f'(\beta)b + W - f'(\beta).\beta - W]'$$

$$= f'(\beta)\, E[(b - \beta)(b - \beta)']\{f'(\beta)\}'$$

$$= f'(\beta)\, \sigma^2 (X'X)^{-1}\{f'(\beta)\}'$$

$$= \sigma^2 f'(\beta)(X'X)^{-1}\{f'(\beta)\}', \qquad (9)$$

From (8) and, (9), the mean squared error (MSE) matrix is

$$MSE(b_G) = V(b_G) + BB'$$

$$= \sigma^2 f(\beta)(X'X)^{-1}\{f'(\beta)\}', + [\{f'(\beta) - I\}\beta + W]$$

$$[\{f'(\beta) - I\}\beta + W]', \qquad (10)$$

Some Remarks

(i) Results of various estimators may be easily seen to be the special cases of this study. For example, the OLS estimator b has $f(\beta) = I$ and $W = 0$ which make the bias expression in (8) 0 showing that b is an unbiased estimator of β. Similarly, for the restricted least squares estimator b_R, we have $f(\beta) = I - (X'X)^{-1}R'[R(X'X)^{-1}R']^{-1}R$ and $W = (X'X)^{-1}R'[R(X'X)^{-1}R']^{-1}r = (X'X)^{-1}R'[R(X'X)^{-1}R']^{-1}R\beta$ (when $r = R\beta$) which, after substituting in the expression in (8), gives the bias $B = 0$ getting as a particular case, the well known result that b_R is unbiased for β when $r = R\beta$.

(ii) For the OLS estimator b, $f'(\beta) = I$ which, when substituted in the general result of variance - covariance matrix of b_G in (9) gives the same variance - covariance matrix $\sigma^2(X'X)^{-1}$ of the OLS estimator b. The restricted least squares estimator b_R has $f(\beta) = I - (X'X)^{-1}R'[R(X'X)^{-1}R']^{-1}R$ which, when substituted in variance - covariance matrix of b_G in (9) gives

$$\sigma^2\{I - (X'X)^{-1}R'[R(X'X)^{-1}R']R\}(X'X)^{-1}\{I - (X'X)^{-1}R'[R(X'X)^{-1}R']^{-1}R\}'$$

$$= \sigma^2(X'X)^{-1} - \sigma^2(X'X)^{-1}R'[R(X'X)^{-1}R']^{-1}R(X'X)^{-1}$$

showing the variance - covariance matrix of b_R given in Johnston[1] as a special case of the variance - covariance matrix of b_G. Also, for the ordinary ridge regression estimator, we have $f'(\beta) = [I + k(X'X)^{-1}]^{-1}$ so that from (9), we get the same expression of the variance - covariance matrix of the ORR estimator

$$\sigma^2[I + k(X'X)^{-1}]^{-1}(X'X)^{-1}[I + k(X'X)^{-1}]^{-1},$$

$$= \sigma^2 (X'X + k I)^{-1} X'X (X'X + k I)^{-1},$$

as mentioned in Johnston[1],

(iii) For the restricted ridge regression (RRR) by Sarkar[3], we have

$$f'(\beta) = [I + k(X'X)^{-1}]^{-1} \{I - (X'X)^{-1}R'[R(X'X)^{-1}R']^{-1}R\}$$

and $$W = [I + k(X'X)^{-1}]^{-1}(X'X)^{-1}R'[R(X'X)^{-1}r$$

which, when substituted in (8) and (9), give the bias vector

$$B = [\{I + k(X'X)^{-1}]^{-1}\{I - (X'X)^{-1}R'[R(X'X)^{-1}R']^{-1}R\} - I]\ \beta$$

$$+ [I + k(X'X)^{-1}]^{-1} \{(X'X)^{-1}R'[R(X'X)^{-1}R']^{-1}r\}$$

$$= [I + k(X'X)^{-1}\beta - \beta \qquad \text{(using } r = R\beta\text{)}$$

$$= -k\,[I + k(X'X)^{-1}]^{-1}(X'X)^{-1}\beta$$

$$= -k\,[(X'X) + k I]^{-1}\beta$$

and the variance - covariance matrix

$$\sigma^2[I+k(X'X)^{-1}\{I-(X'X)^{-1}R'[R(X'X)^{-1}R']^{-1}R\}(X'X)^{-1}\{I-R'[R(X'X)^{-1}R']^{-1}$$

$$R(X'X)^{-1}\}.\ [I + k(X'X)^{-1}]^{-1}$$

$$= \sigma^2(I + k(X'X)^{-1}]^{-1} \{(X'X)^{-1} - (X'X)^{-1}R' [R(X'X)^{-1} R']^{-1}R(X'X)^{-1}\}.$$

$$[I + k(X'X)^{-1}]^{-1}$$

which are the same expressions as obtained by Sarkar[3] and thus showing that the results of Sarkar are special cases of this general study. Results of some more estimators available in the literature may also be shown to be special cases of this study.

References

1 Johnston, J (1991) *Econometric Methods*, 3rd Ed , McGraw - Hill Book Company, P.205, 252.

2. Hoerl, A E & Kennard, R W. (1970) *Technometrics* **12** : 55.

3 Sarkar, N. (1992) *Commun Statist - Theory Meth* **21(7)** . 1987.

PROC. NAT. ACAD. SCI. INDIA, 74 (A), I, 2004

A basic hypergeometric approach to mock theta functions

S. AHMAD ALI

Department of Mathematics, Aamiruddaula Islamia Degree College, Lucknow-226001, India.

Email: aahmad@postmark.net

Received January 16, 2003, Accepted May 2, 2003

Abstract

In this paper it has been shown that all the mock theta functions of order six are the combinations of basic hypergeometric functions. These representations clearly suggest a fresh look *via* a basic hypergeometric transformation theory

(**Keywords** : basic hypergeometric series/mock theta functions)

Introduction

Ramanujan's last gift to the world of mathematics was his mock theta functions, which he reported to G. H. Hardy in his last letter to him.

Definition (Ramanujan) : A mock theta function is a function given by a q-series convergent in $|q|<1$ and *(i)* for which the asymptotic form at *rational singular points exp* $(2\pi ir/s)$ closes as neatly as in the case of theta functions, but (*ii*) which can not be expressed as the sum of an ordinary theta function and a trivial function (a function which is O(1) at all rational points).

Hardy's Version : In Ramanujan's collected paper Hardy[1] wrote "Ramanujan makes it clear that what he meant by a mock theta function. A mock theta function is defined by a q-series convergent when $|q|<1$, for which we can calculate the asymptotic formula, when q tends to a rational point exp $(2\pi ir/s)$, of the same degree of precision as those furnished for the ordinary theta functions by theory of linear transformations".

In his aforesaid last letter, Ramanujan listed a set of seventeen functions classifying them in three groups of order three, five and seven without giving any reason for his classification and he gave the identities connecting these functions

belonging to the same group The discovery of these functions was announced to the mathematical world almost fifteen years after his death by Watson[2] during his celebrated address to the London Mathematical Society in 1935, who also proved all the identities connecting these functions given by Ramanujan. Watson added three more functions and said, "... rather strangely he seems to have overlooked the set of functions $\omega(q)$, $\nu(q)$, $p(q)$". But this statement of Watson was not quite correct since in the 'Lost' Notebook[3] Ramanujan did mention these functions (on pages 15 & 17).

After Watson a number of mathematicians carried the work on them from where Watson had left. In 1966, Andrews[4] generalized most of the known mock theta function identities. Agarwal[5] in 1969 obtained a very general class of basic hypergeometric transformations which themselves contained Andrews results as special cases. There have also been attempts to give alternate definitions to these functions. The most convenient definitions of third order mock theta functions have been given by Fine[6], who gave it in terms of Hein's basic hypergeometric functions.

In 1991, after the discovery of 'Lost' Notebook, Andrews and Hicherson[7] proved eleven identities found in the 'Lost' Notebook connecting seven q-functions, which they called as mock theta functions of order six. They based their classification on some combinatorial consideration, about which Ramanujan never mentioned. As an ample measure of precaution they remarked that they have labeled these functions as of order six as a convenient way of nomenclature.

The methods of Watson[2], Fine[6], Andrews[4] and Agarwal[5&8] make it amply obvious that the structure of all the mock theta functions owes their origin to certain basic hypergeometric functions. With this background in mind the present paper has been aimed at. We have shown that all the mock theta functions of order six are in fact combinations of certain basic hypergeometric functions. These new representations clearly indicate a basic hypergeometric approach, which would not only be more justified but can also be useful.

Notations and Some Known Results

Let, for $|q| < 1$

$$(a;q^k)_n = (1-aq^k)(1-aq^{k+1}) \ldots\ldots\ldots\ldots(1-aq^{k(n-1)}),\ (a;q^k)_0 = 1.$$

$$(a_1,\ a_2,\ldots\ldots\ a_r;q^k)_n = (a_1;aq^k)_n\,(a_2;q^k)_n \ldots\ldots(a_r;q^k)_n$$

A basic hypergeometric series is defined as

$$ {}_{r+1}\Phi_r[a_1,a_2,\ldots,a_{r+1};b_1,b_2,\ldots,b_r;q^k;z] = \sum_{n=0}^{\infty} \frac{\left(a_1,a_2,\ldots a_{r+1};q^k\right)_n z^n}{\left(q,b_1,b_2,\ldots b_r;q^k\right)_n}. $$

The above series converges for $|z| < 1$ and $|q| < 1$. In the above notations, when $k = 1$ we shall omit it from the symbol.

The seven mock theta functions defined by Ramanujan[3] and labeled as of order six by Andrews and Richerson[7] are as follows :

$$ \varphi(q) = \sum_{n=0}^{\infty} \frac{(-1)^n q^{n^2}\left(q;q^2\right)_n}{(-q)_{2n}} \qquad \Psi(q) = \sum_{n=0}^{\infty} \frac{(-1)^n q^{(n+1)^2}\left(q;q^2\right)_n}{(-q)_{2n+1}} $$

$$ \sigma(q) = \sum_{n=0}^{\infty} \frac{q^{(n+1)(n+1)/2}(-q)_n}{\left(q;q^2\right)_{n+1}} \qquad \rho(q) = \sum_{n=0}^{\infty} \frac{q^{n(n+1)/2}(-q)_n}{\left(q;q^2\right)_{n+1}} $$

$$ \lambda(q) = \sum_{n=0}^{\infty} \frac{(-1)^n q^n\left(q;q^2\right)_n}{(-q)_n} \qquad \mu(q) = \sum_{n=0}^{\infty} \frac{(-1)^n (q)_n}{(-q)_n} $$

$$ \nu(q) = \sum_{n=0}^{\infty} \frac{q^{n^2}(q)_n}{\left(q^3;q^3\right)_n} $$

In what follows, we shall make use of the following transformation due to Slater[9].

$$ \sum_{\mu=1}^{D} \prod \left[\begin{matrix} (a)d_\mu,(b)/d_\mu,qd_\mu/z,z/d_\mu \\ (c),(d)/d_\mu \end{matrix} \right] {}_{B+C}\Phi_{A+D-1}\left[(c)d_\mu, qd_\mu/(b);\ (a)d_\mu,qd_\mu/(a);\ Q_\mu\right] $$

$$ = \sum_{\nu=1}^{C} \prod \left[\begin{matrix} (b)c_\nu,(a)/c_\nu,zc_\nu q/zc_\nu,q/zc_\nu \\ (d)c_\nu,(c)/c_\nu \end{matrix} \right] {}_{A+D}\Phi_{B+C-1}\left[(d)c_\nu,\ qc_\nu/(a);\right. $$

$$ \left.(b)c_\nu,qc_\nu/(c);\ Q_\nu\right] \qquad (1) $$

where

$$Q_\mu = (-q^{(n+1)/2} d_\mu)^{D-B-1} \frac{b_1 b_2 ... b_B}{d_1 d_2 .. d_D z}$$

$$Q_\nu = (-q^{(n+1)/2} c_\nu)^{C-A-1} \frac{a_1 a_2 ... a_A q}{c_1 c_2 ... c_C z}$$

Certain new Representation of Mock Theta Functions

We shall now represent the mock theta functions of order six as combinations of basic hypergeometric functions ${}_3\Phi_2$ and ${}_2\Phi_1$

Taking $A = 1$, $B = 0$, $C = 2$, $D = 2$ in (1), we get

$$\frac{(ad_1, qd_1/z, z/d_1)_\infty}{(c_1d_1, c_2d_1, d_2/d_1)_\infty} {}_2\Phi_2[c_1d_1, c_2d_1; ad_1, qd_1/d_2; -q^{(n+1)/2} z/d_2]$$

$$+ \frac{(ad_2, qd_2/z, z/d_2)_\infty}{(c_1d_2, c_2d_2, d_1/d_2)_\infty} {}_2\Phi_2[c_1d_2, c_2d_2; ad_1, qd_2/d_1;\ q^{(n+1)/2} z/d_1]$$

$$= \frac{(a/c_1, zc_1, q/zc_1)_\infty}{(c_1d_1, c_1d_2, c_2/c_1)_\infty} {}_3\Phi_2[c_1d_1, c_2d_2, qc_1/a; 0,\ qc_1/c_2;\ aq/c_1c_2z]$$

$$+ \frac{(a/c_2, zc_2, q/zc_2)_\infty}{(c_2d_1, c_2d_2, c_1/c_2)_\infty} {}_3\Phi_2[c_2d_1, c_2d_2, qc_2/a;\ 0, qc_2/c_1;\ aq/c_1c_2z] \qquad (2)$$

Now in (2) taking $a = q/z$, $c_1 = \sqrt{q/z}$, $d_2 = z\sqrt{q}$, $d_2 = -z$, we get

$$(1+\sqrt{q})\,\rho(q) + q\lambda(q) = \frac{4q(q)_\infty(-q)_\infty^4}{(q^{1/2})_\infty^4(-q^{1/2})_\infty}\,{}_1\Phi_1[q^{1/2};\,-q;\,-q^{n/2}]$$

$$-\frac{q(q)_\infty(-q^{1/2})_\infty^4}{(-q)_\infty(q^{1/2})_\infty^4}\,{}_2\Phi_1[q^{1/2},-q^{1/2};\,0;-q] \qquad (3)$$

Transforming the first series on the right of (2) by using Sears[10] [p. 176], we get

$$(1+\sqrt{q})\,\rho(q) + q\lambda(q) = \frac{4q(q)_\infty(-q)_\infty^4}{(q^{1/2})_\infty^4}\,{}_2\Phi_1[q^{1/2},\,-1;0;\,-q^{1/2}]$$

$$-\frac{q(q)_\infty(-q^{1/2})_\infty^4}{(-q)_\infty(q^{1/2})_\infty^4}\,{}_2\Phi_1[q^{1/2},-q^{1/2};\,0;-q] \qquad (3)$$

where

$$\lambda(q) = {}_3\Phi_2[q,\,q^{1/2},-q^{1/2};\,0,\,q\,;\,-q]$$

Now replacing $q\to q^2$ in (1) and taking $a = 1/z$, $c_1 = -1/z$, $c_2 = -q/z$, $d_1 = -zq$, $d_2 = zq$, we get

$$\frac{(-q,-q^3,-q^{-1};q^2)_\infty}{2(q,q^2,-q^2;q^2)_\infty}\,\varphi(q) + \frac{(q,q^2,q^{-1};q^2)_\infty}{2(-q,-q^2,-q^2;q^2)_\infty}\,{}_1\Phi_1[-q,\,q;\,q^2\,;\,q^n]$$

$$= \frac{4(-q^2;q^2)_\infty^3}{(q,q,-q;q^2)_\infty}\,{}_2\Phi_1[-q^2,-q^2;0;q^2;q]$$

$$+\frac{(-q,-q,-q^{-1};q^2)_\infty}{(q^2,-q^2,-q^{-1};q^2)_\infty}\,{}_3\Phi_2[q^2,-q^2,-q^3;0,\,q^3,\,q^2\,;\,q]$$

Again using Sears[10] [p. 176] in the second series on left, we get

$$\varphi(q) = \frac{8(-q^2;q^2)_\infty^4 (q^2;q^2)_\infty}{(-q;q^2)_\infty^4 (q;q^2)_\infty} {}_2\Phi_1[-q^2,-q^2;0,\ q^2\ ;\ q]$$

$$+\frac{(1-q)(q;q^2)_\infty^4 (q^2;q^2)_\infty^2}{(-q;q^2)_\infty^4 (-q^2;q^2)_\infty} {}_2\Phi_1[0,-1;\ q;\ q^2;\ q]$$

$$-\frac{2q(-q;q^2)_\infty}{(1-q)(-q^3;q^2)_\infty} {}_3\Phi_2[q^2,-q^2,-q^3;\ 0,q^3;\ q^2;\ q] \qquad (5)$$

Replacing $q \to q^2$ in (1) and taking $a = q^2/z$, $c_1 = -q/z$, $c_2 = q^2/z$, $d_1 = -z$, $d_2 = z/q$ and then using Sears[10] [p. 176], we get

$$\psi(q) = \frac{(-q;q^2)_\infty^4, (q^2;q^2)_\infty}{4(q,q^2)_\infty (-q^2;q^2)_\infty} {}_2\Phi_1[-q,-1;\ 0;\ q^2;\ q]$$

$$-\frac{\left(q;q^2\right)_\infty^5 \left(q^2;q^2\right)_\infty}{4\left(-q;q^2\right)_\infty \left(-q^2;q^2\right)_\infty^4} {}_2\Phi_1\ [0,-q;\ q;q^2;q]$$

$$-\frac{2q\left(-q;q^2\right)_\infty}{(1-q)\left(-q^2;q^2\right)_\infty} {}_3\Phi_2\ [-q,\ q^2,-q^2;0,q^3;q^2;\ q] \qquad (6)$$

Similarly on taking a = q^2/z, $c_1 = q^{3/2}/2z$, $c_2 = q^{3/2}/z$, $d_1 = z/\sqrt{q}$, $d_2 = -z/q$ in (1), we get

$$2q^2\sigma(q) + (1-q)^2\mu(q) = q^{-1/2}(1+q^{1/2})(1-q)\frac{(q)_\infty \left(-q^{1/2}\right)_\infty^4}{\left(-q,q^{3/2}\right)_\infty \left(q^{1/2}\right)_\infty^3} {}_2\Phi_1[q^{1/2},-q^{1/2};0;-1]$$

$$-4q^{1/2}\ (1-q)\ \frac{(q)_\infty \left(-q^{1/2}\right)_\infty^4}{\left(-q,q^{3/2}\right)_\infty \left(q^{1/2}\right)_\infty^3}\ {}_2\Phi_1\ [-q,q^{1/2};0;-q^{1/2}] \qquad (7)$$

where

$$\mu(q) = {}_3\Phi_2\,[q,q^{1/2},-q^{1/2};0,-q;-1]$$

Conclusion

From the above analysis, it is more than obvious that mock theta functions of order six have to be treated as simple basic hypergeometric series ${}_3\Phi_2$, ${}_2\Phi_1$ or a combination thereof. This is in conformity with the acknowledged notion that Ramanujan was well conversant with the hypergeometric series and their transformation theory. And therefore in the absence of any complete definition of mock theta functions one has to decide how far it is justified to call these q series as mock theta functions.

It may further be remarked that here we have considered the sixth order mock theta functions of Andrews and Hicherson who themselves as an ample measure of precaution have remarked that the nomenclature sixth order mock theta function may or may not have deeper significance. For us it remains a mystery as to why Ramanujan himself classified the first seventeen as of order three, five and seven in his last letter to Hardy. However to quote Agarwal[11] who has justifiably remarked that "... Ramanunjan's last letter to Hardy is perhaps the longest dying declaration in the mathematical history of the world by one of the greatest mathematician of the last century and hence we accept his classification as true."

Similar basic hypergeometric representations are being attempted with the firm hope for the eight and the tenth order mock theta functions.

Acknowledgment

I thank Professor R. P. Agarwal for his valuable suggestions during the present work. This work has been supported by a research grant no. CST/D-3197 of the Council of Science & Technology, U.P., India.

References

1. Hardy, G. H. (1927) *Collected Papers of Srinivasa Rarnanujan*, Cambridge University Press.
2 Watson, G. N (1936) *J Lon Math. Soc.* **11** : 55.
3 Ramanujan, S. (1988) *The 'Lost' Notebook and other Unpublished Papers*, Narosa Pub. House (New Delhi).

4 Andrews, G E (1966) *Quart J Math* (Oxford) **17** 60

5 Agarwal, R P (1969) *Quart J Math* (Oxford) **20** 121

6 Fine, N J (1988) *Basic Hypergeometric Series and Applications*, AMS Math Survey & Monograph 27.

7 Andrews, G E & Hicherson, D H (1991) *Advan Math* **89** 60.

8 Agarwal, R P (1994) *Proc Nat Acad Sci* (India) **64 A** 95

9 Slater, L J. (1966) *Generalized Hypergeometric Functions*, Cambridge University Press

10 Sears, D B. (1951) *Proc Lond Math Soc* **53** 158

11 Agarwal, R P. (2000) *Proc of Int Conf on Special Functions & their Applications*, Society for Special Functions and their Applications (India) · 11

PROC NAT ACAD SCI. INDIA, 74 (A), I, 2004

Properties of certain fractional q-operators and cut q-Hankel transform

S. AHMAD ALI

Department of Mathematics, Amiruddaula Islamia Degree College, Lucknow-226 001, India.

Email ahmad@postmark.net

Received January 16, 2003, Accepted May 2, 2003

Abstract

In this paper a new cut q-hankel transform has been defined. The relationships between the cut q-Hankel transform, q-Mellin transform has been established with fractional q-integral operators

(**Keywords** fractional q-operators/cut q-Hankel transform/cut q-Bassel function/q-Mellin transform)

Introduction

Al Salam[1] and Agrawal[2] have defined the following two fractional q-integral operators

$$K_q^{\eta,\alpha} f(x) = \frac{q^{-\eta} x^{\eta}}{\Gamma_q(\alpha)} \int_x^{\infty} (t-x)_{\alpha-1}\, t^{-\eta-\alpha} f\left(xq^{-\alpha-k}\right) d_q t \tag{1}$$

and

$$I_q^{\eta,\alpha} f(x) = \frac{x^{-\eta-\alpha}}{\Gamma_q(\alpha)} \int_0^{x} (x-tq)_{\alpha-1}\, t^{\eta} f(t)\, d_q t \tag{2}$$

They have also studied the relationship of these operators with other operators. The object of this paper is to study the relationship of the above operators with q-Mellin transform and a cut q-Hankel transform defined in this paper.

In what follows, we have used the following notations. For $|q| < 1$, we have

$$(q^{\alpha})_n = (1-q^{\alpha})\,(1-q^{\alpha+1})\ldots\,(1-q^{\alpha+n-1}),\ (q^{\alpha})_0 = 1.$$

$$\begin{bmatrix}\alpha\\ k\end{bmatrix}_q = \frac{(1-q^{\alpha})(1-q^{\alpha+1})\ldots(1-q^{\alpha+k-1})}{(q)_k}, \begin{bmatrix}\alpha\\ 0\end{bmatrix}_q = 1.$$

$$(x-y)_{\nu} = x^{\nu}\prod_{n=0}^{\infty}\frac{1-(y/x)q^n}{1-(y/x)q^{\nu+n}}$$

$$\Gamma_q(x) = \frac{(1-q)_{\alpha-1}}{(1-q)^{\alpha-1}},\ \alpha \neq 0, -1, -2,\ldots$$

A basic hypergeometric series is defined as

$${}_r\Phi_s\,[a_1, a_2,\ldots a_r;\ b_1, b_2,\ldots b_s;\ x] = \sum_{n=0}^{\infty}\frac{(a_1)_n(a_2)_n\ldots(a_r)_n\,x^n}{(q)_n(b_1)_n(b_2)_n\ldots(b_s)_n}.$$

We shall denote the first $(m+1)$ terms of the series by ${}_r\Phi_s\,[\ldots]_m$.

A q- integral is defined by means of

$$\int_x^x f(t)d_qt = x(1-q)\sum_{k=1}^{\infty}q^{-k}f\left(xq^{-k}\right)$$

$$\int_0^x f(t)d_qt = x(1-q)\sum_{k=1}^{\infty}q^{k}f\left(xq^{k}\right)$$

$$\int_0^{\infty} f(t)d_qt = (1-q)\sum_{k=-\infty}^{\infty}q^{k}f\left(q^{k}\right)$$

provided the series on the right converges. Also, in sequel, it is assumed that the function $f(x)$ are such that

$$\sum_{k=-\infty}^{\infty} \left| q^k f\left(\alpha q^k\right) \right|$$

converges for all $\alpha > 0$.

In these notations the fractional q-integral operators given by (1) and (2) can be written as

$$K_q^{\eta,\alpha} f(x) = (1-q)^{\alpha} \sum_{k=0}^{\infty} (-1)^k q^{k(\eta+\alpha)+k(k+1)/2} \begin{bmatrix} -\alpha \\ k \end{bmatrix}_q f\left(xq^{-\alpha-k}\right) \tag{3}$$

$$I_q^{\eta,\alpha} f(x) = \frac{(1-q)}{\Gamma_q(\alpha)} \sum_{k=0}^{\infty} q^{k(1+\eta)} \left(1-q^{k+1}\right)_{\alpha-1} f\left(xq^k\right) \tag{4}$$

which are valid for all α. Lastly, we define the q-Mellin transform by means of q-integral

$$M_q^s f(x) = \int_0^{\infty} x^{s-1} f(x)\, d_q t \tag{5}$$

$$= (1-q) \sum_{k=-\infty}^{\infty} q^{ks} f(q^k)$$

and the q-Bessel function is defined as

$$J_{q,\nu}(x) = \frac{(x/2)^{\upsilon}}{(1-q)_{\nu}} {}_2\Phi_1 \left[0,\ 0;\ q^{\nu+1};\ -x^2/4\right].$$

Some Properties of Operators (1) and (2)

In this section we study an interesting relation between fractional q-operators (1), (2) and q-Mellin transform (5)

Theorem : Whenever the series involved are absolutely convergent, we have

$$M_q^{s} K_q^{\eta,\alpha} f(x) = \frac{(1-q)^{\alpha}}{\left(q^{1+\eta+s}\right)_{\alpha}} M_q^{s+1} f(xq^{-\alpha}) \tag{6}$$

$$M_q^{s} I_q^{\eta,\alpha} f(x) = \frac{(1-q)^{\alpha}}{\left(q^{1+\eta-s}\right)_{\alpha}} M_q^{s+1} f(x) \tag{7}$$

Proof of (6) : From (1) and (5) , we have

$$M_q^{s} K_q^{\eta,\alpha} f(x) = \int_0^{\infty} x^{s-1} K_q^{\eta+\alpha} f(x) d_q x$$

$$= (1-q) \sum_{t=-\infty}^{\infty} q^{ts} K_q^{\eta,\alpha} f(q^t)$$

$$= (1-q)^{\alpha+1} \sum_{t=-\infty}^{\infty} q^{ts} \sum_{k=0}^{\infty} (-1)^k q^{k(\eta+\alpha)+k(k+1)/2} \begin{bmatrix} -\alpha \\ k \end{bmatrix}_q f(q^{\alpha-k+t})$$

Simplification and the change of order of summation gives

$$M_q^{s} K_q^{\eta,\alpha} f(x) = (1-q)^{\alpha+1} \sum_{r=-\infty}^{\infty} q^{rs} f\left(q^{-\alpha+r}\right) \sum_{k=0}^{\infty} \frac{\left(q^{\alpha}\right)_k}{(q)_k} \left(q^{1+\eta+s}\right)^k$$

$$= \frac{(1-q)^{\alpha+1} \left(q^{1+\eta+s+\alpha}\right)_{\infty}}{\left(q^{1+\eta+s}\right)_{\infty}} \sum_{r=-\infty}^{\infty} q^{rs} f\left(q^{-\alpha+r}\right)$$

$$= \frac{(1-q)^{\alpha}}{\left(q^{1+\eta+s}\right)_{\infty}} \int_0^{\infty} x^{s} f(xq^{-\alpha}) d_q x$$

$$= \frac{(1-q)^{\alpha}}{\left(q^{1+\eta+s}\right)_{\infty}} M_q^{s+1} f(xq^{-\alpha})$$

Proof of (7) Using (1) and (5), we write

$$M_q^s I_q^{\eta,\alpha} f(x) = \int_0^{\infty} x^{s-1} I_q^{n\alpha} f(x)\, d_q x.$$

$$= \frac{(1-q)^2}{\Gamma_q(\alpha)} \sum_{t=-\infty}^{\infty} q^{st} \sum_{k=-\infty}^{\infty} q^{k(1+\eta)} (1-q^{k+1})_{\alpha-1} f(q^{k+t})$$

Changing the order of integration and simplifying, we get

$$M_q^s I_q^{\eta,\alpha} f(x) = \frac{(1-q)^2 (q)_{\infty}}{\Gamma_q(\alpha)\left(q^{\alpha}\right)_{\infty}} \sum_{r=-\infty}^{\infty} q^{rs} f(q^r) \sum_{k=0}^{\infty} \frac{\left(q^{\alpha}\right)_k}{(q)_k} (q^{1+\eta-s})^k$$

$$= \frac{(1-q)(q)_{\infty}\left(q^{1+\eta+\alpha-s}\right)_{\infty}}{\Gamma_q(\alpha)\left(q^{\alpha}\right)_{\infty}\left(q^{1+\eta-s}\right)_{\infty}} \int_0^{\infty} x^s f(x)\, d_q x$$

$$= \frac{(1-q)^{\alpha}}{\left(q^{1+\eta-s}\right)_{\alpha}} M_q^{s+1} f(x)$$

This completes the proof.

A Cut q-Hankel Transform and the Operators (1) and (2)

We now introduce the cut q-Hankel transform by means of the following q-integral

$$H_{q,\nu,m} f(x) = \int_0^{\infty} J_{q,\nu,m}\left(2\sqrt{xy}\right) f(y)\, d_q y \qquad (8)$$

where $J_{q,\nu,m}(x)$ is a cut Bassel function defined as

$$J_{q,\nu,m}(x) = \frac{(x/2)^{\upsilon}}{(1-q)_{\nu}} {}_2\Phi_1 [\ 0,\ 0;\ q^{\nu+1};\ -x^2/4]_m$$

The ordinary case of the cut Hankel transform has been extensively studied by Erdelyi[3] and Kober[4,5] in a series of papers. Owing to its importance in a number of physical problems, it is worthwhile to study the corresponding properties of (8), which may have some application in discrete problems.

We now give below the result in the form of theorem for our new operator (8).

Theorem : Whenever the series involved converges absolutely, we have

$$K_q^{\nu/2,\alpha} H_{q,\nu+2\alpha,m} f(x) = \frac{(1-q^{\alpha})(q)_{\infty}}{(1-q)_{\nu+2\alpha}(q^{1-\alpha})_{\infty}} (xq^{-1})^{\alpha(\nu/2+\alpha)} M_q^{\alpha+1}(x^{1+\nu/2} f(x)) \quad (10)$$

$$I_q^{\nu/2,\alpha} H_{q,\nu,m} f(x) = \frac{(1-q^{\alpha})(1-q)_{\nu+\alpha}}{(1-q)_{\nu}(q^{1+\nu})_{\infty}} x^{-\alpha/2} H_{q,\nu,m}(x^{-\nu/2} f(x)). \quad (11)$$

Proof of (10) : From (1) and (8), we have

$$K_q^{\nu/2,\alpha} H_{q,\nu+2,m} f(x) = (1-q)^{\alpha} \sum_{k=0}^{\infty} (-1)^k q^{k(\nu/2+\alpha)+k(k+1)/2} \begin{bmatrix} -\alpha \\ k \end{bmatrix}_q H_{q,\nu+2\alpha,m} f(xq^{-\alpha-k})$$

$$= (1-q)^{\alpha+1} \sum_{k=0}^{\infty} \frac{(q^{1+\nu/2})^k (q^{\alpha})_k}{(q)_k} \sum_{t=-\infty}^{\infty} q^t J_{q,\nu+2\alpha,m}\left(2\sqrt{xq^{-\alpha-k+t}}\right)$$

On simplification the right hand side becomes

$$\frac{(1-q)^{\alpha+1}(q)_{\infty}}{(1-q)_{\nu+2\alpha}(q^{1-\alpha})} (xq^{-1})^{\alpha(\nu/2+\alpha)} \sum_{t=-\infty}^{\infty} q^{t(1+\nu/2+\alpha)} f(q^t)$$

$$= \frac{(1-q)^{\alpha+1}(q)_\infty}{(1-q)_{\nu+2\alpha}(q^{1-\alpha})_\infty}(xq^{-1})^{\alpha(\nu/2+\alpha)} \int_0^\infty x^{1+\nu/2+\alpha} f(x)\, d_q(x)$$

$$= \frac{(1-q)^{\alpha+1}(q)_\infty}{(1-q)_{\nu+2\alpha}(q^{1-\alpha})_\infty}(xq^{-1})^{\alpha(\nu/2+\alpha)}\ M_q^{\alpha+1}(x^{1+\nu/2} f(x))$$

Proof of (11) : Again from (2) and (8), we have

$$I_q^{\nu/2,\alpha} H_{q,\nu,\nu} f(x) = \frac{x^{\nu/2}}{\Gamma_q(\alpha)} \int_0^x (x-yq)_{\alpha-1}\, y^{\nu/2}\, H_{q,\nu+2,m} f(t)\, d_q(y)$$

$$= \frac{(1-q)}{\Gamma_q(\alpha)} \sum_{k=0}^{\infty} q^{k(1+\nu/2)} (1-q^{k+1})_{\alpha-1}\, H_{q,\nu,m} f(xq^k)$$

$$= \frac{(1-q)^2(q)_\infty}{\Gamma_q(\alpha)(q^\alpha)_\infty} \sum_{k=0}^{\infty} \frac{q^{k(1+\nu/2)}(q^\alpha)_k}{(q)_k} \sum_{t=-\infty}^{\infty} q^t J_{q,\nu,m}\left(2\sqrt{xq^{k+t}}\right) f(q^t)$$

On simplification the right hand side becomes

$$\frac{(1-q)^{\alpha-1} x^{\nu/2}}{(1-q)_\nu (q^{1+\nu})_\infty} \sum_{t=-\infty}^{\infty} q^{t(1+\nu/2)} f(q^t)\ {}_2\Phi_1\,[0,\ 0;\ q^{1+\alpha+\nu};\ -xq^t]_m$$

$$= \frac{(1-q)^\alpha (1-q)_{\nu+\alpha} x^{-\alpha/2}}{(1-q)_\nu (q^{1+\nu})_\infty} H_{q,\nu,m}(x^{-\nu/2} f(x))$$

This completes the proof of the theorem.

In a recent communication we propose to study the q-cut Bassel function defined in this paper.

Acknowledgment

This work has been supported by a research grant no. CST/D-3197 of the Council of Science & Technology, U.P., India.

References

1 Al Salam, W (1966) *Proc Edin Math Soc* **15** 135

2 Agarwal, R P (1969) *Proc Comb Phil Soc* **66** 365

3 Erdelyi, A (1940) *Quart J Math (Oxford)* **11** . 293

4 Kober, H & Erdelyi, A (1940) *Quart. J Math (Oxford)* **11** . 212

5 Kober, H (1940) *Quart J Math (Oxford)* **11** · 113

PROC. NAT. ACAD. SCI. INDIA, 74 (A), I, 2004

Thermal stresses due to contact of a hot ring with long aelotropic cylinder

BISWAJIT DATTA and B. DAS*

Computer Centre, North Bengal University, Darjeeling, West Bengal, India.

**Department of Mathematics, North Bengal University, Darjeeling, West Bengal, India.*

Received August 16, 2001; Revised July 10, 2002; Accepted November 9, 2002

Abstract

This paper deals with the generation of thermal stresses when a long cylinder is in contact with a hot ring on its outer surface. Isotropic cases have been considered by several authors but here we deal with a long non-isotropic cylinder taking into consideration of the stress-strain relations in the presence of temperature. This is axisymmetric thermoelastic problem.

(**Keywords** : thermal stress/axisymmetric/aelotropic/thermal strain/radial stress)

Introduction

Thermal-stress problems for isotropic solids have been taken into considerations by many authors determining the steady-state thermal stresses in an isotropic long cylinder due to hot ring in contact with its outer surface. This problem is concerned with the determination of thermal stresses corresponding to a long non-isotropic cylinder. A particular material magnesium is considered here calculating thermal stresses in radial direction numerically. Axis of the cylinder is taken as the axis of symmetry.

Method of Solution

It is convenient to use cylindrical co-ordinates (r, θ, z) so that considering the axially symmetric character of the problem, the nonvanishing component of stress-tensors are ($r\hat{r}, \theta\hat{\theta}, z\hat{z}, r\hat{z}$)

For axisymmetric character of the problem, the corresponding strain components are[2]

$$(e_{rr})_T = \frac{\partial u_T}{\partial r}, (e_{\theta\theta})_T \frac{u_T}{r}, (e_{zz})_T = \frac{\partial w_T}{\partial z}, (e_{rz})_T = \frac{1}{2}\left(\frac{\partial u_r}{\partial z} + \frac{\partial w_T}{\partial r}\right)\Bigg] \tag{1}$$

where are the components of displacement due to temperature. Substituting (1) the stress-strain relations in presence of temperature[1], we get

$$\left.\begin{aligned}
(rr)_T &= C_{11}\frac{\partial u_T}{\partial r} + C_{12}\frac{u_T}{r} + C_{11}\frac{\partial w_T}{\partial z} - a_1 T, \\
(\theta\theta)_T &= C_{12}\frac{\partial u_l}{\partial r} + C_{11}\frac{u_r}{r} + C_{13}\frac{\partial w_T}{\partial z} - a_1 T, \\
(zz)_T &= C_{13}\frac{\partial u_T}{\partial r} + C_{13}\frac{u_T}{r} + C_{33}\frac{\partial w_T}{\partial z} - a_2 T, \\
(rz)_T &= C_{44}\left(\frac{\partial u_T}{\partial z} + \frac{\partial w_T}{\partial z}\right)
\end{aligned}\right] \tag{2}$$

Substituting (2) in the equations of equilibrium we have

$$\left.\begin{aligned}
C_{11}\left(\frac{\partial^2 u_T}{\partial r^2} + \frac{1}{r}\frac{\partial u_T}{\partial r} - \frac{u_T}{r^2}\right) + (C_{13} + C_{44})\frac{\partial^2 w_T}{\partial r \partial z} + C_{44}\frac{\partial^2 u_T}{\partial z^2} &= a_1 \frac{\partial T}{\partial r} \\
C_{44}\left(\frac{\partial^2 w_T}{\partial r^2} + \frac{1}{r}\frac{\partial w_T}{\partial r}\right) + (C_{13} + C_{44})\left(\frac{\partial^2 u_T}{\partial r \partial z} + \frac{1}{r}\frac{\partial u_T}{\partial z}\right) + C_{33}\frac{\partial^2 w_T}{\partial z^2} &= a_1 \frac{\partial T}{\partial z}
\end{aligned}\right\} \tag{3}$$

We have heat conduction equation in the steady state[3]

$$\nabla_1^2 T = 0 \tag{4}$$

where

$$\nabla_1^2 = \frac{\partial^2}{\partial r^2} + \frac{1}{r}\frac{\partial}{\partial r} + k^2 \frac{\partial^2}{\partial z^2}$$

k being a constant depending on the ratio of the conductivity coefficients.

Let us choose the components of displacement as

$$u_T = \lambda \frac{\partial \phi}{\partial_T}, w_T = \mu \frac{\partial \phi}{\partial z} \tag{5}$$

where $\phi = \phi(r, \theta, z)$ and λ, μ are constants.

Putting (5) in (3) and rearranging we get

$$\left.\begin{aligned} C_{11}\lambda\left(\frac{\partial^2\phi}{\partial r^2}+\frac{1}{r}\frac{\partial\phi}{\partial r}\right)+\left[\lambda C_{44}+\mu(c_{13}+C_{44})\right]\frac{\partial^2\phi}{\partial z^2} &= a_1 T \\ \left[C_{44}\mu+\lambda(C_{13}+C_{44})\right]\left(\frac{\partial^2\phi}{\partial r^2}+\frac{1}{r}\frac{\partial\phi}{\partial r}\right)+C_{13}\mu\frac{\partial^2\phi}{\partial z^2} &= a_2 T \end{aligned}\right\} \tag{6}$$

which are satisfied if

$$\nabla_1^2 \phi = 0 \tag{7}$$

$$k^2 \frac{\partial^2 \phi}{\partial z^2} = T \tag{8}$$

and if the constants λ and μ are related by the relation

$$\left.\begin{aligned} \lambda(C_{44}-k^2C_{11})+\mu(C_{13}+C_{44}) &= a_1k^2 \\ -\lambda k^2(C_{13}+C_{44})+(C_{33}+C_{44}k^2) &= a_1k^2 \end{aligned}\right\} \tag{9}$$

Solving (9) for λ and μ,

$$\left.\begin{aligned} \lambda &= \frac{a_1k^2(C_{33}-C_{44}k^2)-a_2(C_{13}+C_{44})}{C_{11}C_{44}k^2+(C_{13}^2-C_{11}C_{33}+2C_{13}C_{44})+C_{33}C_{44}} \\ \mu &= \frac{k^2a_1k^2\left[(C_{13}+C_{44})+a_2(C_{44}-C_{11}k^2)\right]}{C_{11}C_{44}k^2(C_{13}^2-C_{11}C_{33}+2C_{13}C_{44})+C_{33}C_{44}} \end{aligned}\right\} \tag{10}$$

Let us take the solution of (7) as[4]

$$\phi = \int_{-\infty}^{\infty} f(m).mI_0(mr)\cos\left(\frac{mz}{k}\right)dm \tag{11}$$

where $I_0\,(mr)$ is the modified Bessel function[5] of the first kind and zero order.

So from (8), we get

$$T = -\int_{-\infty}^{\infty} m^3 f(m).I_0(mr)\cos\left(\frac{mz}{k}\right)dm \tag{12}$$

So, the components of displacement and stress due to temperature derived from (5) and (1) are

$$U_T = 2\lambda\int_0^{\infty} m^2 f(m).I_1(mr)\cos\left(\frac{mz}{k}\right)dm$$

$$w_T = -2\frac{\mu}{k}\int_0^{\infty} m^2 f(m).I_0(mr)\sin\left(\frac{mz}{k}\right)dm$$

$$(rr)_T = 2\left(a_1 + C_{11}\lambda - \frac{C_{13}\mu}{k^2}\right)\int_0^{\infty} m^3 f(m).\,I_0\,(mr)\cos\left(\frac{mz}{k}\right)dm + \frac{2\lambda(C_{12}-C_{11})}{r}\int_0^{\infty} m^2 f(m).\,I_1\,(mr)\cos\left(\frac{mz}{k}\right)dm$$

$$(\theta\theta)_T = 2\left(a_1 + C_{12}\lambda - \frac{C_{13}\mu}{k^2}\right)\int_0^{\infty} m^2 f(m).\,I_0(mr)\cos\left(\frac{mz}{k}\right)dm + \frac{2\lambda\,(C_{11}-C_{12})}{r}\int_0^{\infty} m^2 f(m).\,I_1(mr)\cos\left(\frac{mz}{k}\right)dm$$

$$(zz)_T = 2\left(a_2 + C_{13}\lambda - \frac{C_{33}\mu}{k^2}\right)\int_0^{\infty} m^3 f(m).\,I_0(mr)\cos\left(\frac{mz}{k}\right)dm,$$

$$(rz)_T = -2\,C_{44}\,\frac{\lambda+\mu}{k}\int_0^{\infty} m^3 f(m).I_1(mr)\sin\left(\frac{mz}{k}\right)dm \tag{13}$$

Complementary Solution

For rotational symmetry of the stresses and displacements, the non-vanishing stress-components are $(rr)_c$, $(\theta\theta)_c$, $(zz)_c$, and $(rz)_c$, the subscript determines complementary stresses without temperature.

The stress-strain relations without temperature are

$$\left.\begin{aligned}(rr)_c &= C_{11}(e_{rr})_c + C_{12}(e_{\theta\theta})_c + C_{13}(e_{zz})_c\\ (\theta\theta)_c &= C_{12}(e_{rr})_c + C_{11}(e_{\theta\theta})_c + C_{13}(e_{zz})_c\\ (zz)_c &= C_{13}(e_{rr})_c + C_{13}(e_{\theta\theta})_c + C_{33}(e_{zz})_c\\ (rz)_c &= C_{44}(e_{rz})_c\end{aligned}\right\} \tag{14}$$

where

$$(e_{rr})_c = \frac{\partial \mu_e}{\partial r},\ (e_{\theta\theta})_c = \frac{u_e}{r},\ (e_{zz})_c = \frac{\partial w_e}{\partial z},\ (e_{rz})_c = \frac{1}{2}\left(\frac{\partial u_c}{\partial z} + \frac{\partial w_e}{\partial r}\right), \tag{15}$$

u_c and w_c are components of displacement in r and z directions respectively.

Let,

$$u_c = \frac{\partial \phi}{\partial r}\quad w_c = s\frac{\partial \phi}{\partial z},\ \text{where } s \text{ is arbitrary} \tag{16}$$

Using (16) on (15) and putting those values in equation of equilibrium in absence of body force, we get

$$\left.\begin{aligned}C_{11}\left(\frac{\partial^2 \psi}{\partial r^2} + \frac{1}{r}\frac{\partial \psi}{\partial r}\right) + [C_{44} + s(C_{13} + C_{14})]\frac{\partial^2 \psi}{\partial z^2} &= 0\\ (C_{13} + C_{44} + s\,C_{44})\left(\frac{\partial^2 \psi}{\partial r^2} + \frac{1}{r}\frac{\partial \psi}{\partial r}\right) + s\,C_{33}\frac{\partial^2 \psi}{\partial z^2} &= 0\end{aligned}\right\} \tag{17}$$

Non-trivial solution of two equations of (17) requires them identical, for which we have

$$\frac{s\left(C_{13}+C_{44}\right)+C_{44}}{C_{11}}=\frac{s\,C_{33}}{s\,C_{44}+C_{13}+C_{44}}\equiv p^2\,(\text{say}) \tag{18}$$

Eliminating s from (18) we derive an equation

$$C_{11}C_{44}p^4+\left(2C_{13}C_{44}+C_{13}^2-C_{11}C_{33}\right)p^2+C_{33}C_{44}=0 \tag{19}$$

which yields two roots p_1^2 and p_2^2 are real in case of magnesium but are conjugate imagineries for zinc.

So, we get the displacement of the form

$$\left.\begin{aligned} u_c &= \frac{\partial}{\partial r}\left(\psi_1+\psi_2\right)\\ w_3 &= \frac{\partial}{\partial z}\left(p_1^2\,\psi_1+p_2^2\psi_2\right)\end{aligned}\right\} \tag{20}$$

where ψ_1 and ψ_2 are the solutions of

$$\left(\frac{\partial^2}{\partial r^2}+\frac{1}{r}\frac{\partial}{\partial r}+p_i^2\frac{\partial^2}{\partial z^2}\right)\psi_i=0\ ,\ i=1,2. \tag{21}$$

Now, we take the solution for (20) in the form

$$\psi_1=\int_0^\infty mf_1(m)\,I_0\left(\frac{mp_1}{k}r\right)\cos\frac{mz}{k}\,dm,\quad \psi_2=\int_0^\infty mf_2(m)\,I_0\left(\frac{mp_2}{k}r\right)\cos\frac{mz}{k}\,dm, \tag{22}$$

when arbitrary $f_1(m)$ and $f_2(m)$ being functions of m are to be determined from the boundary conditions.

With the help of (22), the displacement components (20) become

$$\left.\begin{aligned} u_c &= \frac{1}{k}\int_0^\infty m^2\left[p_1 f_1(m) I_1\left(\frac{mp_1}{k}r\right) + p_2 f_2(m) I_1\left(\frac{mp_2}{k}r\right)\right]\cos\left(\frac{mz}{k}\right)dm \\ w_c &= -\frac{1}{k}\int_0^\infty m^2\left[p_1 f_1(m) I_0\left(\frac{mp_1}{k}r\right) + p_2^2 f_2(m) I_0\left(\frac{mp_2}{k}r\right)_1\right]\sin\left(\frac{mz}{k}\right)dm \end{aligned}\right\} \quad (23$$

Using u_c and w_c from (23) in (15) and putting these components of strain in stress-strain relations (14) we obtain

$$\begin{aligned} (\widehat{rr})_c &= \frac{C_{11}-C_{13}}{k^2}\int_0^\infty m^3\left[p_1^2 f_1(m) I_0\left(\frac{mp}{k}r\right) + p_2^2 f_2(m) I_0\left(\frac{mp_2}{k}r\right)\right]\cos\left(\frac{mz}{k}\right)dm \\ &+ \frac{C_{12}-C_{11}}{rk}\int_0^\infty m^3\left[p_1 f_1(m) I_1\left(\frac{mp_1}{k}r\right) + p_2 f_2(m) I_1\left(\frac{mp_2}{k}r\right)_1\right]\cos\left(\frac{mz}{k}\right)dm, \\ (\widehat{\theta\theta})_c &= \frac{C_{12}-C_{13}}{k^2}\int_0^\infty m^3\left[p_1^2 f_1(m) I_0\left(\frac{mp_1}{k}r\right) + p_2^2 f_2(m) I_0\left(\frac{mp_2}{k}r\right)\right]\cos\left(\frac{mz}{k}\right)dm \\ &+ \frac{C_{11}-C_{12}}{rk}\int_0^\infty m^3\left[p_1 f_1(m) I_1\left(\frac{mp_1}{k}r\right) + p_2 f_2(m) I_1\left(\frac{mp_2}{k}r\right)_1\right]\cos\left(\frac{mz}{k}\right)dm, \\ (\widehat{zz})_c &= \frac{C_{13}-C_{33}}{k^2}\int_0^\infty m^3\left[p_1^2 f_1(m) I_0\left(\frac{mp_1}{k}r\right) + p_2^2 f_2(m) I_0\left(\frac{mp_2}{k}r\right)\right]\cos\left(\frac{mz}{k}\right)dm \\ (rz)_c &= \frac{C_{44}}{k^2}\int_0^\infty m^3\left[p_1\left(1+p_1^2\right) f_1(m) I_1\left(\frac{mp_1}{k}r\right) + p_2\left(1+p_2^2\right) f_2(m) I_1\left(\frac{mp_2}{k}r\right)\right]\cos\left(\frac{mz}{k}\right)dm \end{aligned} \quad (24)$$

The resultant stresses are given by

$$\left.\begin{aligned} rr &= (rr)_T + (rr)_c \\ \theta\theta &= (\theta\theta)_T + (\theta\theta)_c \\ zz &= (zz)_T + (zz)_c \\ rz &= (rz)_T + (rz)_c \end{aligned}\right\} \quad (25)$$

In order that the boundary surface of the cylinder may be free from the radial and shear stresses, we have on $r = a$,

$$\left.\begin{aligned}(rr)_{r=a} &= 0\\ (rz)_{z=a} &= 0\end{aligned}\right\} \tag{26}$$

From (26) we have when $r = a$,

$$p_1 f_1(m)\left[ap_1(C_{11}-C_{13})I_0\left(\frac{mp_1}{k}a\right)+(C_{12}-C_{11})I_1\left(\frac{mp_1}{k}a\right)\right]$$

$$+p_2 f_2(m)\left[ap_2(C_{11}-C_{13})I_0\left(\frac{mp_2}{k}a\right)+k(C_{12}-C_{11})I_1\left(\frac{mp_2}{k}a\right)\right]$$

$$+2f(m)\left[a\left(a_1k^2+C_{11}\lambda k^2-C_{13}\mu\right)I_0(ma)+\frac{\lambda(C_{12}-C_{11})}{m}k^2 I_1(ma)\right]=0,$$

and

$$p_1(1+p^2)I_1\left(\frac{mp_1}{k}a\right)f_1(m)+p_2\left(1+p_2^2\right)I_1\left(\frac{mp_2}{k}a\right)f_2(m)+2k(\lambda+\mu)I_1(ma)f(m)=0$$

Solving these two equation for $f_1(m)$ and $f_2(m)$,

$$\left.\begin{aligned}f_1(m) &= \frac{2f(m)}{p_1}\cdot\frac{\Delta_1(m)}{\Delta_3(m)}\\ f_2(m) &= \frac{2f(m)}{p_2}\cdot\frac{\Delta_2(m)}{\Delta_3(m)}\end{aligned}\right\}$$

where

$$\Delta_1(m)=k(\lambda+\mu)I_1(ma)\left[ap_2(C_{11}-C_{13})I_0\left(\frac{mp_2}{k}a\right)+k(C_{12}-C_{11})I_1\left(\frac{mp_2}{k}a\right)\right]$$

$$\left[a\left(a_1k^2+C_{11}\lambda k^2-C_{13}\mu\right)I_0\,(ma)+\frac{\lambda\left(C_{12}-C_{11}\right)}{m}k^2I_1(ma)\right],$$

$$\Delta_2(m)=\left(1+p_1^2\right)I_1\left(\frac{mp_1}{k}a\right)\left[a\left(a_1k^2+C_{11}\lambda k^2-C_{13}\mu\right)I_0(ma)\frac{\lambda\left(C_{12}-C_{11}\right)}{m}k^2I_1(ma)\right]$$
$$-k(\lambda+\mu)I_1(ma)\left[ap_1(C_{11}-C_{13})I_0\left(\frac{mp_1}{k}a\right)+k(C_{13}-C_{11})I_1\left(\frac{mp_1}{k}a\right)\right]$$

and

$$\Delta_3(m)=\left(1+p_2^2\right)I_1\left(\frac{mp_2}{k}a\right)\left[ap_1(C_{11}-C_{13})\,I_0\left(\frac{mp_1}{k}a\right)+(C_{12}-C_{11})I_1\left(\frac{mp_1}{k}a\right)\right]$$
$$-1\left(1+p_1^2\right)I_1\left(\frac{mp_1}{k}a\right)\left[ap_2(C_{11}-C_{13})\,I_0\left(\frac{mp_2}{k}a\right)+k(C_{12}-C_{11})\,I_1\left(\frac{mp_2}{k}a\right)\right]$$

With these values of $f_1(m)$ and $f_2\ (m)$ the resultant stresses from (25) and components of displacement from (23) are formally known keeping only unknown quantity $f(m)$.

Temperature Distribution

For the distribution of stress, produced in the cylinder by the nuclei of thermoelastic strain, T_0 being along the circle $r = a, z = 0$. We assume

$$T = T_0\,\delta(z) \qquad \text{on } r = a$$

where $\delta(z)$ is the Dirac delta function. So we get from (12)

$$-\int_{-\infty}^{\infty}m^3 f(m)\ I_0\ (ma)\cos\left(\frac{mz}{k}\right)dm=\frac{T_0}{k}\int_{-\infty}^{\infty}\cos\frac{mz}{k}dm.$$

or, $T_0 = -m^3 f(m)\ I_0\ (ma)$

or $f(m) = -\dfrac{T_0}{m^3 I_0(ma)}$

Thus the problem in completely solved For numerical evaluation, we consider from (25),

$$(rr)_{z=0} = [(rr)_I + (rr)_c]_{z=0}$$

$$=2(a_1+C_{11}\lambda - \frac{C_{13}\mu}{k^2}) \int_{-\infty}^{\infty} m^3 f(m)\, I_1(mr)\, dm$$

$$+\frac{2\lambda(C_{12}-C_{11})}{r}\int_0^{\infty} m^2 f(m)\, I_1(mr)\, dm$$

$$+\frac{(C_{11}-C_{13})}{k^2}\int_0^{\infty} m^3\left[p_1^2 f_1(m) I_0\left(\frac{mp_1}{k}r\right)+p_2^2 f_2(m) I_0\left(\frac{mp_2}{k}r\right)\right] dm$$

$$+\frac{(C_{12}-C_{11})}{rk}\int_0^{\infty} m^3\left[p_1 f_1(m) I_1\left(\frac{mp_1}{k}r\right)+p_2 f_2(m) I_1\left(\frac{mp_2}{k}r\right)\right] dm.$$

Numerical Results

The roots of (19) are real for magnesium so we take elastic constants of the material[6] for $a = 1$ and $k = 1$,

$$\left.\begin{aligned} &C_{11} = 0.565\times10^{12}\text{dyne/cm}^2, C_{12} = 0.232\times10^{12}\text{dyne/cm}^2, C_{13} = 0.181\times10^{12}\text{dyne/cm}^2, \\ &C_{33} = 0\ 587\times10^{12}\text{dyne/cm}^2, C_{44} = 0.168\times10^{12}\text{dyne/cm}^2 \end{aligned}\right\}$$

The coefficients of linear thermal expansion are

$$\alpha_1 = 27.7 \times 10^{-6}\text{cm/}0^0\ C,\ \alpha_2 = 26.6\times 10^{-6}\text{cm/}0^0\ \text{C}$$

The roots p_1^2, p_2^2 of (19) are $p_1^2 = 1.63$ and $p_2^2 = 0.64$

$a_1 = 26.8915 \times 10^6$, $a_2 = 25.6414 \times 10^6$, $\lambda = -51.8656 \times 10^{-6}$, $\mu = 17.7762 \times 10^{-6}$

With these values we get the radial stress when $z = 0$,

$$\frac{10^{-6}(rr)_{z=0}}{T_0}\,dynes/cm^2\,0^0\,C = 11.2602\int_0^\infty \frac{I_0(mr)}{I_0(m)}dm - \frac{34.5425}{12}dm - \int_0^\infty \frac{I_0(mr)}{I_0(m)}dm$$

$$-\int_0^\infty \frac{1}{I_0(m)\,\Delta_3(m)}\left[\Delta_1(m)\,I_0(1.2768\,mr) + 6.125\,\Delta_2(m)\,I_0(0.08\,mr)\right]dm$$

when

$$\Delta_1(m) = 10^6\left[9.23271\,I_0(m)\,I_1(0.8m) + \left(11.3518 - \frac{28.3248}{m}\right)\right.$$

$$\left.\times\, I_1(m)\,I(0.08m) - 1.04651 I_1(m)\,I_0(0.08m)\right],$$

$$\Delta_2(m) = 2.63\,I_1(1\,2768m)\times 10^6$$

$$\left[\left(26.8915 - 0.565\times 51.8656 - 0.181\times 17.7762\right)I_0(m) + \frac{51.8656}{m}\times 0.333 I_1(m)\right]$$

$$+34.0894\times 10^6\,I_1(m)[1\,2768\times 0.3841 I_0(1.2768m) - 0.333\,I_1(1.2768m)]$$

$$\Delta_3(m) = 10^{12}\,[I_1(0.08m)\,\{0.8025 I_0(1.2768m) - 0.5461 I_1(1.2768m)\}$$

$$- I_1(1\,2768m)\,\{0.0807 I_0(0.08m) - 0.8758 I_1(0.08m)\}]$$

Finally the distribution of axial stress with r is provided in the table below :

r (cm)	0	0 2	0 4	0 6	0 8
$\frac{10^{-10}(r\hat{r})_{z=0}}{T_0 \text{dynes/cm}^2\,0^0\text{C}}$	1.9233	1.9239	1 9313	1 9472	1 9569

References

1 Sharma, B D (1958) *Jour of Applied Mechanics* **25** : 86

2 Nowacki, W (1986) *Thermoelasticy,* 2nd Ed. Pergamon Press, London, p - 17

3. Carslaw, H S & Jaeger, J C (1957) *Conduction of heat in solids,* 2nd Ed Oxford University Press, p - 214

4 Sternberg, E. & Mcdowell, E.L (1957) *Qly of Appl Math* **14** . 4

5 Watson, G N. (1952) *A Treatise on the Theory of Bassel Functions,* 2nd Ed Cambridge University Press, London

6 Hearmon, R F S (1946) *Rev Modern Phys* **18** 409

Regd. No. R.N. 35621/78

CONTENTS

Published by Dr. V.P. Kamboj, General Secretary for the National Academy of Sciences, India, Allahabad and printed by National Graphics, Allahabad.
Managing Editor – Professor S.L Srivastava